Accepted Manuscript

The concept of hybrid molecules of tacrine and benzyl quinolone carboxylic acid (BQCA) as multifunctional agents for Alzheimer's disease

V. Hepnarova, J. Korabecny, L. Matouskova, P. Jost, L. Muckova, M. Hrabinova, N. Vykoukalova, M. Kerhartova, T. Kucera, R. Dolezal, E. Nepovimova, K. Spilovska, E. Mezeiova, N.L. Pham, D. Jun, F. Staud, D. Kaping, K. Kuca, O. Soukup

PII: S0223-5234(18)30226-5

DOI: 10.1016/j.ejmech.2018.02.083

Reference: EJMECH 10260

To appear in: *European Journal of Medicinal Chemistry*

Received Date: 15 August 2017

Revised Date: 9 February 2018

Accepted Date: 27 February 2018

Please cite this article as: V. Hepnarova, J. Korabecny, L. Matouskova, P. Jost, L. Muckova, M. Hrabinova, N. Vykoukalova, M. Kerhartova, T. Kucera, R. Dolezal, E. Nepovimova, K. Spilovska, E. Mezeiova, N.L. Pham, D. Jun, F. Staud, D. Kaping, K. Kuca, O. Soukup, The concept of hybrid molecules of tacrine and benzyl quinolone carboxylic acid (BQCA) as multifunctional agents for Alzheimer's disease, *European Journal of Medicinal Chemistry* (2018), doi: 10.1016/j.ejmech.2018.02.083.

The Concept of Hybrid Molecules of Tacrine and Benzyl Quinolone Carboxylic Acid (BQCA) as Multifunctional Agents for Alzheimer´s Disease

Hepnarova V[#], Korabecny J[#], Matouskova L, Jost P, Muckova L, Hrabinova M, Vykoukalova N, Kerhartova M, Kucera T, Dolezal R, Nepovimova E, Spilovska K, Mezeiova E, Pham N L, Jun D, Staud F, Kaping D, Kuca K, Soukup O

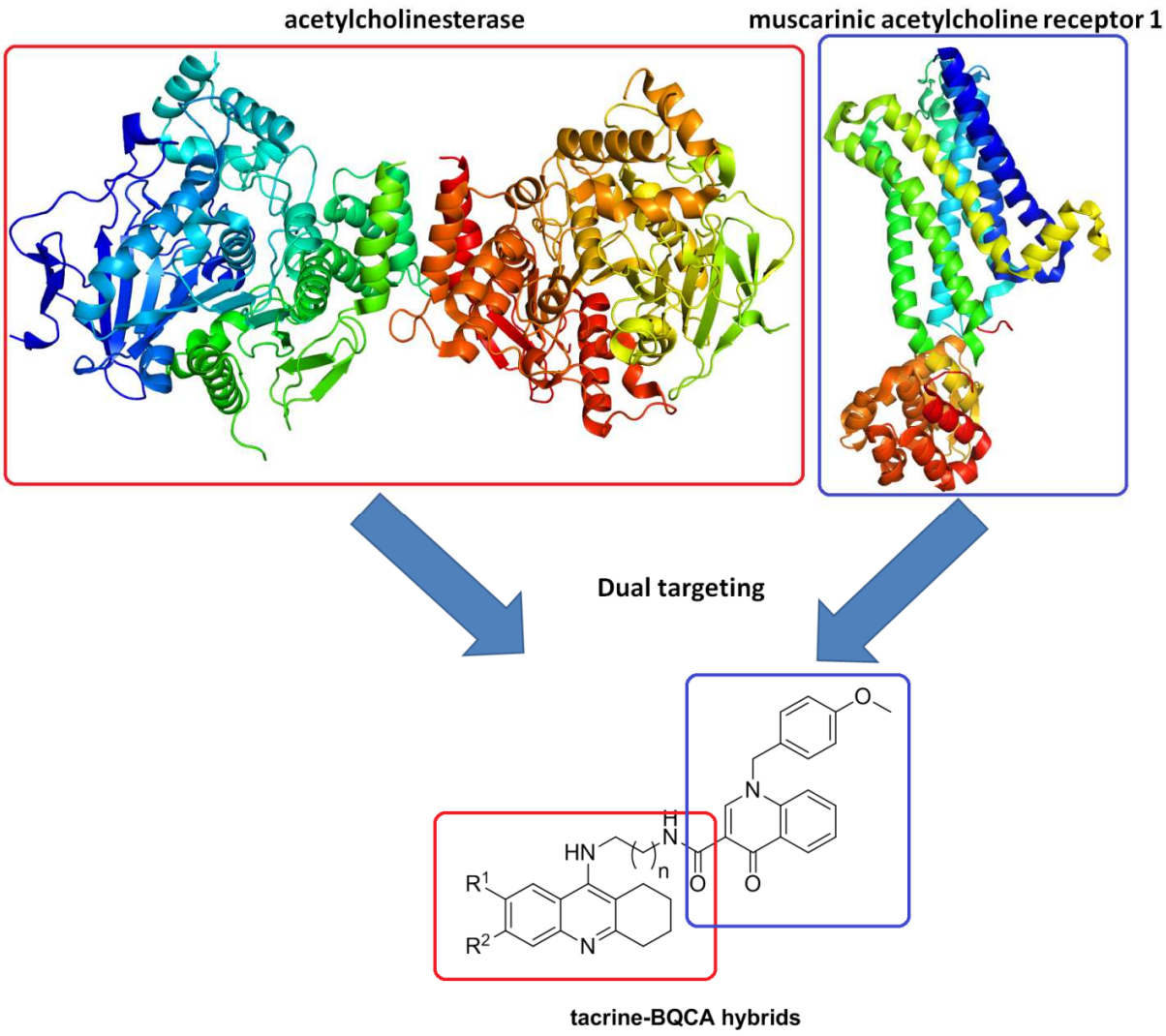

The Concept of Hybrid Molecules of Tacrine and Benzyl Quinolone Carboxylic Acid (BQCA) as Multifunctional Agents for Alzheimer´s Disease

Hepnarova V[1,2#], Korabecny J[1,2#], Matouskova L[1], Jost P[1], Muckova L[1], Hrabinova M[1,2], Vykoukalova N[4], Kerhartova M[4], Kucera T[1], Dolezal R[2], Nepovimova E[1,2,5], Spilovska K[2,3], Mezeiova E[2,3], Pham N L[1,2], Jun D[1,2], Staud F[4], Kaping D[3], Kuca K[2,5], Soukup O[2,*]

[1] Department of Toxicology and Military Pharmacy, Faculty of Military Health Sciences, University of Defence, Trebesska 1575, 500 01 Hradec Kralove, Czech Republic

[2] Biomedical Research Centre, University Hospital, Sokolska 581, 500 05 Hradec Kralove, Czech Republic

[3] National Institute of Mental Health, Topolova 748, 250 67 Klecany, Czech Republic

[4] Department of Pharmacology, Department of Pharmaceutical Chemistry and Drug Control, Faculty of Pharmacy, Charles University, Heyrovskeho 1203, 500 05 Hradec Kralove, Czech Republic

[5] Department of Chemistry, Faculty of Science, University of Hradec Kralove, Rokitanskeho 62, 500 03 Hradec Kralove, Czech Republic

# contributed equally

[*] corresponding author e-mail address: osoukup83@gmail.com

ABSTRACT

Novel tacrine-benzyl quinolone carboxylic acid (tacrine-BQCA) hybrids were designed based on multi-target directed ligands (MTLDs) paradigm, synthesized and evaluated *in vitro* as inhibitors of human acetylcholinesterase (*h*AChE) and human butyrylcholinesterase (*h*BChE). Tacrine moiety is represented herein as 7-methoxytacrine, 6-chlorotacrine or unsubsituted tacrine forming three different families of seven members, i.e. 21 compounds in overall. Introducing BQCA, a positive modulator of M1 muscarinic acetylcholine receptors (mAChRs), the action of novel compounds on M1 mAChRs was evaluated via Fluo-4 NW assay on the Chinese hamster ovarian (CHO-M1WT2) cell line. All the novel tacrine-BQCA hybrids were able to block the action of *h*AChE and *h*BChE in micromolar to nanomolar range. The *h*AChE kinetic profile of **5p** was found to be mixed-type which is

consistent with our docking experiments. Moreover, selected ligands were assessed for their potential hepatotoxicity on HepG2 cell line and presumable permeation through the blood-brain barrier by PAMPA assay. Expected agonistic profile towards M1 mAChRs delivered by BQCA moiety was not confirmed. From all the hybrids, **5o** can be highlighted as non-selective cholinesterase inhibitor (*h*AChE IC_{50} = 74.5 nM; *h*BChE IC_{50} = 83.3 nM) with micromolar antagonistic activity towards M1 mAChR (IC_{50} = 4.23 μM). Non-selective pattern of cholinesterase inhibition is likely to be valuable during the onset as well as later stages of AD.

Key words: 7-methoxytacrine, acetylcholinesterase, acetylcholinesterase inhibitor, butyrylcholinesterase, Alzheimer´s disease, BQCA, multi-target directed ligands, positive allosteric modulator of muscarinic receptor, tacrine

1. INTRODUCTION

Alzheimer´s disease (AD) is an irreversible, progressive neurodegenerative brain disorder known to affect adults 65 years and older. Although no AD disease-modifying therapy is currently available, diverse drug candidates are intensively investigated to slow the worsening of dementia symptoms and improve quality of life for Alzheimer's patients.

One approach is targeting misfolded proteins such as β-amyloid or τ-protein representing the major pathological changes of the disease [1]. Other approaches extensively pursue the reduction of oxidative damage in cell structures, chelation therapy to deal with abnormal metal ion homoeostasis or drugs affecting divergent enzymatic systems such monoamine oxidase, histamine receptors, *N*-methyl-D-aspartate receptors etc. [2–5]. All of the above outlined new therapeutics target the abundant pathology to play a significant role in AD etiology; notwithstanding, that the major cause of AD is not fully understood.

An increasing amount of evidence highlight the loss of cholinergic innervation in the basal forebrain and hippocampus to cause the decline in memory and learning functions in AD patients. In the so-called cholinergic hypothesis firstly postulated by Bartus and colleagues in 1982, the emerging role of acetylcholine (ACh) neurotransmitter laid the foundation for AD treatment exploiting acetylcholinesterase (AChE, E.C. 3.1.1.7) inhibitors (AChEIs) [6]. Accordingly, several AChEIs such as tacrine, donepezil, rivastigmine and galantamine (Fig. 1) have been marketed [7]. Besides, *N*-methyl-D-aspartate receptor (NMDAR) antagonist memantine (Fig. 1) has been approved to repel AD via decrease in excessive glutamate activation of NMDARs [8].

In 1993, tacrine (9-amino-1,2,3,4,-tetrahydroacridine, THA) was approved by the US Food and Drug Administration as the first AChEI for AD treatment [9]. However, THA's hepatotoxicity limited its further use. Nowadays, THA is still largely used as a versatile tool for designing multi-target ligands

(MTDLs) to better cope with the multifactorial nature of AD [10–12] When built in MTDLs, THA confers AChE inhibition properties to the final hybrids. Surprisingly, THA hybridization mostly results in the reduction of toxicity and amplification of the biological profile.

In the context of the multifactorial AD , the M1 subtype of muscarinic ACh receptors (M1 mAChRs) is viewed as a suitable target, since the M1 mAChR is an important subtype for memory and attention mechanisms [13–15]. M1 mAChR stimulation does not only improve cognitive deficit, but also can decrease τ-protein hyperphosphorylation via the activation of protein kinase C and inhibition of glycogen synthase kinase 3β (GSK-3β) [16]. M1 agonists could not only provide symptomatic relief by enhancing cholinergic transmission but also have disease modifying outcomes by influencing amyloid precursor protein (APP) processing [17–19]. The latter effect can be ascribed to mediation of APP processing via non-amyloidogenic pathway releasing soluble APP alpha (sAPPα) [20], thus, deterring the formation of Aβ peptides and slowing AD progression [21]. Unfortunately, difficulties associated with the development of highly selective M1 receptor agonist are due to the highly conserved sequence homology among the orthosteric ACh binding site of mAChR subtypes [21]. The proposed solution for M1 selective ligands appears in targeting less conserved allosteric binding sites hereby providing the specificity for the M1 subtype.

Merck Research Laboratories developed in this context benzylquinolone carboxylic acid (BQCA; 1-(4-methoxybenzyl)-4-oxo-1,4-dihydroquinoline-3-carboxylic acid, Fig. 1). While BQCA does not interact with the ACh site of M1 mAChRs it is well-known as a highly selective positive allosteric modulator of the given receptor subtype. It has subtle effect on other four mAChR subtypes at concentrations up to 100 μM [22]. *In vivo* research showed that BQCA acts pro-cognitively by reversing scopolamine-induces memory deficits [21].

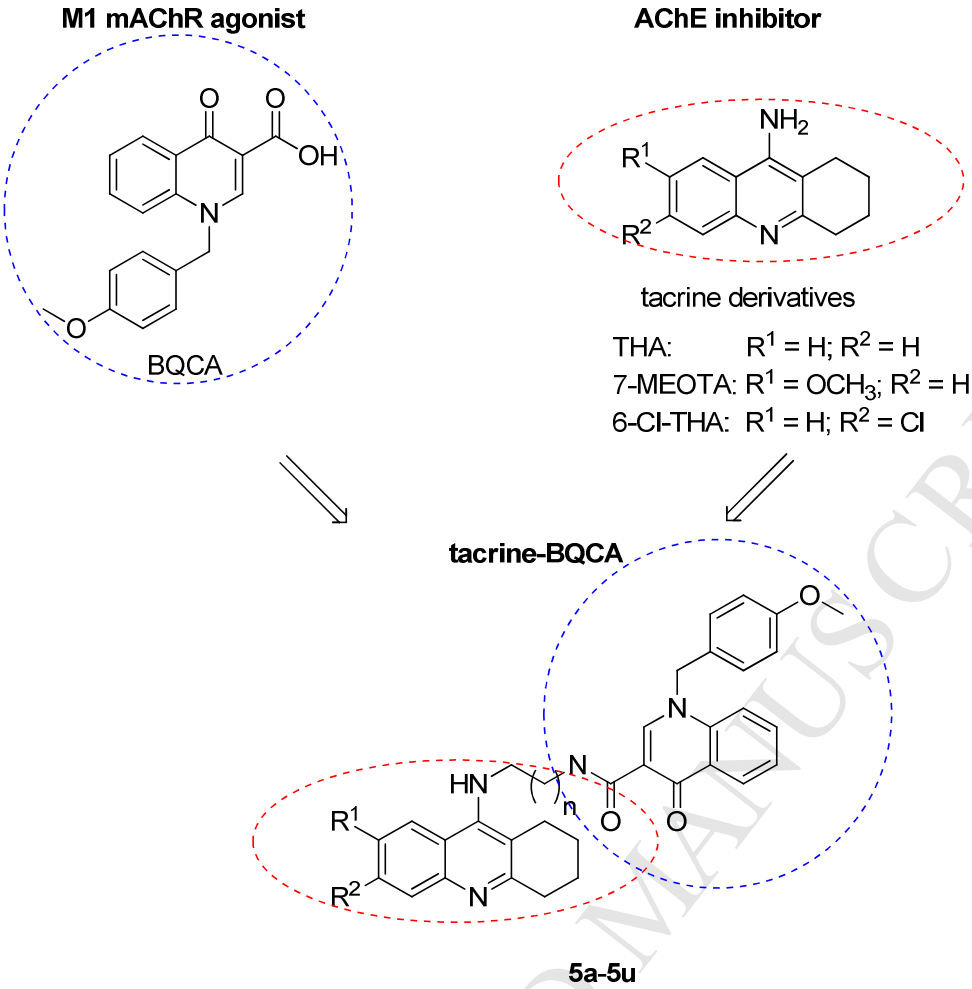

Fig. 1. Design of novel tacrine-BQCA hybrids as potential AChE inhibitor with M1 mAChR agonist.

2. DESIGN OF NOVEL TACRINE-BQCA HYBRIDS

All the aforementioned results directed us to design, synthesize and evaluate novel tacrine-benzyl quinolone carboxylic acid (tacrine-BQCA) hybrids to repel AD (Fig. 1). In this work, we utilized our experiences from MTDLs field in AD [11,23,24]. The rational for combining tacrines with BQCA results from the rational that tacrine moieties would be responsible for AChE inhibition whereas BQCA scaffold would deliver M1 receptor agonist properties [21].

These two pharmacologically distinct entities have been connected by the alkyl spacer of varying lengths into one molecule. As a result, based on tacrine core variants, we have obtained three different families. The first group is represented by THA-BQCA hybrids. The second subset contains 6-chlorotacrine (6-Cl-THA) that has proven 25-fold higher affinity over THA to AChE [25]. Lastly, we have implemented 7-methoxytacrine (7-MEOTA) into the third set yielding 7-MEOTA-BQCA hybrids. The rational for 7-MEOTA implementation is that it exhibits reduced hepatotoxicity while preserving the THA pharmacological profile [26,27]. However, THA shows multimodal and complex action itself

[28]. Beyond cholinesterase inhibition, THA or its derivatives have been found to interact with several other targets related to AD like blockade of M2 subtype of mAChRs, potentiation of brain nicotinic receptors at low doses and inhibition of NMDA receptors [4]. Further, THA has been reported to enhance neurotransmitter release of 5-hydroxytryptamine, noradrenaline, dopamine and GABA [29]. In addition, it shows non-selective monoamine oxidase A/B (MAO-A/B) inhibition [30].

The concept for embodying AChEI and M1 mAChR agonist into a single molecule have already been reported [31]. In this case, hybrids linking M1 mAChR receptor agonist xanomeline with AChEI tacrine via 10 to 17 carbon spacer showed interesting pharmacological profile. Indeed, THA-xanomeline hybrids retained similar or even higher ability to inhibit AChE compared to THA. In addition, these hybrids displayed enhanced M1 allosteric affinity explored using orthosteric radioligand [^{3}H]*N*-methylscopolamine as a probe. Furthermore, THA-xanomeline hybrids´ effect was determined *in vivo* in scopolamine-induced amnesia model in rats resulting in memory improvement out-balancing solely cholinesterase inhibition.

Taken together, in this article we report on the anticholinesterase properties of novel tacrine-BQCA hybrids; paying attention to their behavior pattern towards M1 mAChR. Moreover, their cytotoxicity, *in silico* binding to AChE/butyrycholinesterase (BChE) and CNS availability have been tested.

3. RESULTS AND DISCUSSION

3.1. Chemistry

The synthetic route of the proposed tacrine-BQCA hybrids is illustrated in Schemes 1 and 2. In order to obtain one of the parent compounds, we initially underwent a four step synthesis affording BQCA in 19 % overall (Scheme 1). This included slightly modified reaction conditions of the earlier described synthetic procedure [32]. The first step consisted in reaction of aniline with diethyl ethoxymethylenemalonate by the so-called Gould-Jacobs condensation yielding 1,3-diethyl 2-[(phenylamino)methylidene]propanedioate (**1**) in 90 % [33]. Cyclo-condensation of **1** in diphenylether afforded ethyl 4-oxo-1,4-dihydroquinoline-3-carboxylate (**2**) in 26 %. Benzylation of **2** with 1-(bromomethyl)-4-methoxybenzene resulted in ethyl ester of BQCA (ethyl 1-[(4-methoxyphenyl)methyl]-4-oxo-1,4-dihydroquinoline-3-carboxylate; **3** in 84 %) which in subsequent step, basic ester hydrolysis, turned to 1-[(4-methoxyphenyl)methyl]-4-oxo-1,4-dihydroquinoline-3-carboxylic acid (BQCA, 99 %).

Pursuing the MTDLs strategy to obtain the desired compounds, we fused two frameworks of differently substituted tacrines with BQCA, employing linking approach. A set of diaminotacrines (**4a**-**4u**) were obtained following previously reported procedure [23]. Coupling reaction of **4a**-**4u** with

BQCA catalyzed by benzotriazol-1-yloxy)tris(dimethylamino)phosphonium hexafluorophosphate (BOP) afforded final products **5a**-**5u** (Scheme 2). The identity and purity of **5a**-**5u** was confirmed by high-resolution mass spectrometry and NMR (given in Experimental section and Supporting Information).

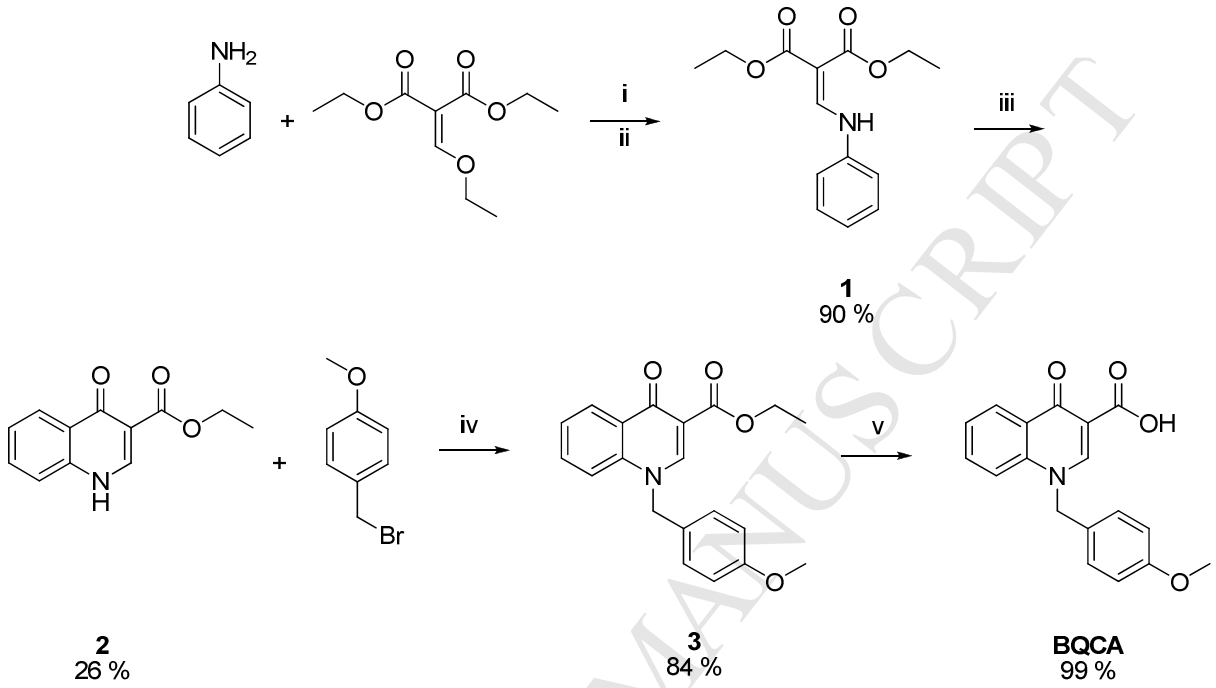

Scheme 1. Synthesis of BQCA as a building block. Reaction conditions: i) neat, RT to 165°C for 6h; ii) 1M HCl, RT to 115°C; iii) diphenylether, 228-232°C, overnight; iv) K_2CO_3 anh., 95°C, KI in DMF, 24h; v) LiOH, water/MeCN, RT, overnight.

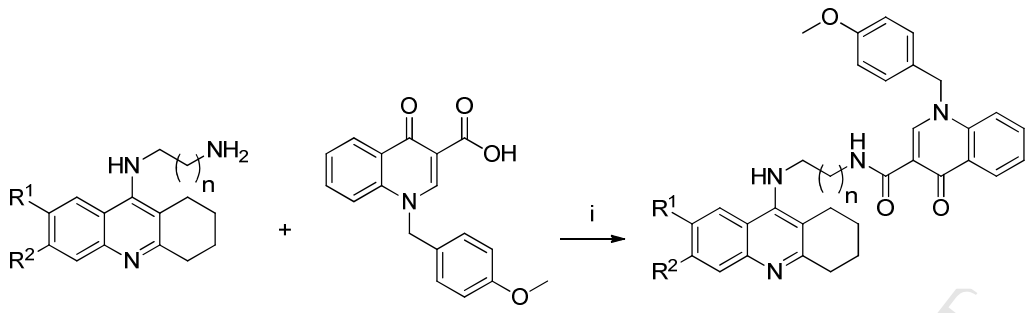

4a-4u **BQCA** **5a-5u**

4a: $R^1 = OCH_3$, R^2 = H; n = 1
4b: $R^1 = OCH_3$, R^2 = H; n = 2
4c: $R^1 = OCH_3$, R^2 = H; n = 3
4d: $R^1 = OCH_3$, R^2 = H; n = 4
4e: $R^1 = OCH_3$, R^2 = H; n = 5
4f: $R^1 = OCH_3$, R^2 = H; n = 6
4g: $R^1 = OCH_3$, R^2 = H; n = 7
4h: R^1, R^2 = H; n = 1
4i: R^1, R^2 = H; n = 2
4j: R^1, R^2 = H; n = 3
4k:R^1, R^2 = H; n = 4
4l: R^1, R^2 = H; n = 5
4m: R^1, R^2 = H; n = 6
4n: R^1, R^2 = H; n = 7
4o: R^1 = H, R^2 = Cl; n = 1
4p: R^1 = H, R^2 = Cl; n = 2
4q: R^1 = H, R^2 = Cl; n = 3
4r: R^1 = H, R^2 = Cl; n = 4
4s: R^1 = H, R^2 = Cl; n = 5
4t: R^1 = H, R^2 = Cl; n = 6
4u: R^1 = H, R^2 = Cl; n = 7

5a: $R^1 = OCH_3$, R^2 = H; n = 1
5b: $R^1 = OCH_3$, R^2 = H; n = 2
5c: $R^1 = OCH_3$, R^2 = H; n = 3
5d: $R^1 = OCH_3$, R^2 = H; n = 4
5e: $R^1 = OCH_3$, R^2 = H; n = 5
5f: $R^1 = OCH_3$, R^2 = H; n = 6
5g: $R^1 = OCH_3$, R^2 = H; n = 7
5h: R^1, R^2 = H; n = 1
5i: R^1, R^2 = H; n = 2
5j: R^1, R^2 = H; n = 3
5k: R^1, R^2 = H; n = 4
5l: R^1, R^2 = H; n = 5
5m:R^1, R^2 = H; n = 6
5n: R^1, R^2 = H; n = 7
5o: R^1 = H, R^2 = Cl; n = 1
5p: R^1 = H, R^2 = Cl; n = 2
5q: R^1 = H, R^2 = Cl; n = 3
5r: R^1 = H, R^2 = Cl; n = 4
5s: R^1 = H, R^2 = Cl; n = 5
5t: R^1 = H, R^2 = Cl; n = 6
5u: R^1 = H, R^2 = Cl; n = 7

Scheme 2. Synthesis of novel tacrine-BQCA hybrids. Reaction conditions: i) DMF, inert atmosphere, RT, TEA, BOP.

3.2. Biochemical evaluation

3.2.1. In vitro AChE and BChE inhibition assay

The inhibitory activities against human AChE (*h*AChE) and human BChE (*h*BChE) of new tacrine-BQCA hybrids, together with those of the THA, 7-MEOTA and 6-Cl-THA, taken as references and BQCA, are reported in Table 1. The activities are expressed as IC_{50} values. All three families were found to be potent inhibitors of cholinesterases with IC_{50} values ranging from micromolar to two digit nanomolar concentration scale. The most active AChE inhibitors in each family were found as follows, **5f**, **5i** and **5p** with the IC_{50} values 1.5 μM, 0.13 μM and 42 nM from 7-MEOTA-BQCA, THA-BQCA and 6-Cl-THA-BQCA subsets, respectively. The general observation can be made between series with descending *h*AChE affinity from 7-MEOTA-BQCA > THA-BQCA > 6-Cl-THA-BQCA. This trend is in agreement with previously published literature for tacrine-trolox hybrids or tacrine-naphthoquinone derivatives [23,34]. Moreover, these findings are consistent with the tested template tacrines, where 6-Cl-THA was found to be the most active *h*AChE inhibitor followed by THA and 7-MEOTA [25,26,35,36]. Note that, BQCA did not show AChE inhibition ability in the tested concentration scale.

The linker between two basic pharmacophores plays a crucial role in contacting both anionic sites which are 20 Å distanced from each other [37]. The firstly described dual-binder, namely bis-7-

tacrine, showed optimal tether size consisting of seven methylene groups [38]. Whereas literature offers many examples of more shortly-linked dimers such as tacrine-naphthoquinone with n = 2-3 [34], or longer-bridged hybrids such as THA-tianeptines hybrids where n = 10-11 [39] or 7-MEOTA-*p*-anisidine hybrids with optimal linker spacer of n= 9 [40]. This may vary depending on the ligand distribution in the enzyme cavity. Considering this, we inspected the optimal linker length between appropriate tacrine and BQCA moieties. In the group of 7-MEOTA-BQCA (**5a**-**5g**) the highest activity was maintained in two and three carbon tethered hybrids (**5a** and **5b**). Elongation of the chain yielded in hybrids with lower inhibition capability with exception displayed by **5f**. This is plausibly produced by the inversion of the binding mode in the *h*AChE active site where 7-MEOTA resides at the rim of the *h*AChE gorge and BQCA is accommodated proximally (see Molecular Modeling Studies). In THA-BQCA series (**5h**-**5n**), the most pronounced *h*AChE inhibitory activity is associated with the derivatives bearing two or three methylene units in the linker (**5h** and **5i**). Similarly, for 6-Cl-THA-BQCA family (**5o**-**5u**), **5p** bearing three methylenes proved to be the most active against *h*AChE. It has to be noted that some derivatives with n = 6 and n = 7 from THA-BQCA (**5l** and **5m**) as well as 6-Cl-THA-BQCA (**5s** and **5t**) families displayed inhibitory activity in the same order of magnitude as the highlighted compounds **5i** and **5p**. These differences might be explained by the plasticity of *h*AChE active site and suitable lodging of BQCA in contacting either mid-gorge region or PAS region of *h*AChE [10,41].

Several lines of evidence suggest that BChE is able to hydrolyze ACh in AChE-knockout mice, displaying a compensatory role when AChE levels are depleted [42,43]. In the brain of patients suffering from AD, BChE co-localizes with AChE contributing to cerebral cortex neurodegeneration in the form of insoluble fibrils, known as senile plaques[44]. In view of these facts, we inspected *h*BChE inhibition by novel tacrine-BQCA hybrids. All the ligands under the survey demonstrated low micromolar to two digits nanomolar *h*BChE inhibition power highlighting **5a** (IC_{50} = 0.41 μM), **5h** (IC_{50} = 59 nM) and **5o** (IC_{50} = 83 nM) from 7-MEOTA-BQCA, THA-BQCA and 6-Cl-THA-BQCA, respectively, as the most potent. These findings are in line with the activity of template tacrine structures where the decreasing order in *h*BChE affinity can be outlined as THA > 6-Cl-THA > 7-MEOTA. Again, the size of the linker between pharmacophores affected the inhibitory activity, revealing that two-carbon tethered hybrids have the highest inhibition power in all three subsets. This findings agree with previously published results of the tacrine-naphthoquinones family [34]. The slightly suppressed affinity of 6-Cl-THA-BQCA family compared to THA is presumably explained by the docking experiments (see below) [45].

From a pharmacological point of view, the AChE/BChE selectivity issue needs to be clarified. Based on the line of reasoning outlined above, prevailing AChE inhibition may support the AD patients at the

onset stages of the disease. In contrast, it is plausible that late stage AD patients have a higher benefit from non-selective or BChE-selective inhibitors. However, to date there is no clear consensus whether it is better to use AChE-selective, BChE-selective or non-selective inhibitors [46]. Accordingly, some hybrids from tacrine-BQCA family preferentially inhibit *h*BChE over *h*AChE (Table 1). Indeed, the top-three ranked *h*AChE selective inhibitors were **5u** (SI for *h*AChE = 312), **5s** (SI for *h*AChE = 142) and **5p** (SI for *h*AChE = 89) all being the members of 6-Cl-THA-BQCA family. Surprisingly, the selectivity inversion can be found predominantly in 7-MEOTA-BQCA subset where hybrids **5c** (SI for *h*AChE = 0.114), **5a** (SI for *h*AChE = 0.155) and **5g** (SI for *h*AChE = 60.167) yielded as the most *h*BChE selective.

Table 1 Inhibitory potencies of tested compounds towards cholinesterases and M1 mAChR expressed as IC_{50} ± SEM (n=3)

Compound	*h*AChE IC_{50} ± SEM (μM)[a]	*h*BChE IC_{50} ± SEM (μM)[a]	Selectivity ratio for *h*AChE[b]	M1 mAChR IC_{50} ± SEM (μM)
7-MEOTA	10.0 ± 1.0	17.6 ± 0.8	1.76	3.71 ± 0.16
THA	0.320 ± 0.013	0.0881 ± 0.0013	0.275	13.0 ± 1.2
6-Cl-THA	0.0176 ± 0.0005	1.73 ± 0.10	98.3	6.09 ± 0.57
BQCA	>1000	>1000	n.d.[c]	n.d.[d]
5a	2.64 ± 0.14	0.408 ± 0.023	0.155	3.71 ± 0.31
5b	2.24 ± 0.09	1.03 ± 0.03	0.460	2.48 ± 0.24
5c	9.50 ± 0.89	1.08 ± 0.07	0.114	1.07 ± 0.26
5d	8.02 ± 0.90	6.16 ± 0.49	0.768	1.37 ± 0.18
5e	10.0 ± 1.4	16.6 ± 2.09	1.66	8.61 ± 1.40
5f	1.53 ± 0.16	49.3 ± 10.4	32.2	11.4 ± 3.06
5g	74.3 ± 17.2	12.4 ± 0.9	0.167	7.86 ± 0.84
5h	0.187 ± 0.007	0.0589 ± 0.0012	0.315	0.658 ± 0.087
5i	0.129 ± 0.004	0.674 ± 0.030	5.23	0.455 ± 0.061
5j	0.491 ± 0.027	1.32 ± 0.04	2.69	1.59 ± 0.19
5k	0.293 ± 0.015	0.823 ± 0.018	2.81	1.48 ± 0.14
5l	0.194 ± 0.007	0.280 ± 0.014	1.44	1.49 ± 0.11
5m	0.194 ± 0.008	1.19 ± 0.06	6.13	2.14 ± 0.27
5n	0.768 ± 0.041	1.28 ± 0.04	1.67	2.05 ± 0.14
5o	0.0745 ± 0.0031	0.0833 ± 0.0050	1.12	4.23 ± 0.66
5p	0.0419 ± 0.0011	3.72 ± 0.13	88.8	4.01 ± 0.26
5q	0.0896 ± 0.0029	3.12 ± 0.26	34.8	4.11 ± 0.31
5r	0.180 ± 0.011	7.74 ± 0.57	43.0	3.27 ± 0.22
5s	0.0941 ± 0.0040	13.4 ± 1.0	142	2.78 ± 0.30
5t	0.0517 ± 0.0034	3.34 ± 0.25	64.6	5.35 ± 0.63
5u	0.119 ± 0.007	37.2 ± 2.16	312	9.45 ± 0.76

[a] Compound´s concentration required to decrease enzyme activity by 50%; the values are the mean ± SEM of three independent measurements, each performed in triplicate; [b] Selectivity for *h*AChE is

determined as ratio *h*BChE IC_{50}/*h*AChE IC_{50}; [c] Not determined; [d] Not determined, BQCA showed agonist profile toward M1 mAChR (see Supplementary information)

3.2.2. Kinetic analysis of *h*AChE inhibition

To assess the interactions of **5p** (as the most potent *h*AChE inhibitor) of the series, a kinetic study was performed. Enzyme velocity curves were recorded at various concentrations of substrate (acetylthiocholine) and tested compound.

The type of *h*AChE inhibition was derived from the non-linear regression analysis, where results for each type model of inhibition (competitive, non-competitive, uncompetitive and mixed) were compared with sum-of-squares *F*-test. Analysis indicated mixed type of inhibition ($p < 0.05$), consistent with graphical representation of Lineweaver–Burk plot (Fig. 2). The same mode of inhibition was described for its parent compound - tacrine [47].

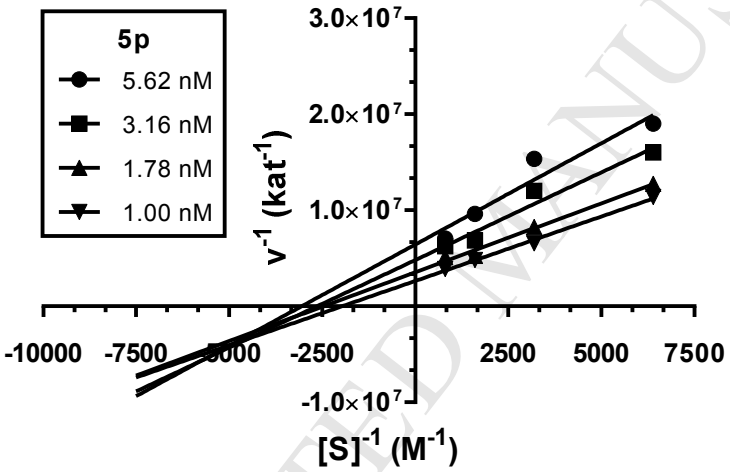

Figure 2. Steady-state inhibition of *h*AChE hydrolysis of substrate acetylthiocholine by compound **5p** at different concentrations. Lineweaver−Burk plots of initial velocity at increasing substrate concentrations (0.156 - 1.250 mM) are presented. Lines were derived from a linear regression of the data points.

The intersection of lines below the x-axis shows higher affinity of **5p** to the enzyme-substrate complex to free enzyme ($K_i > K_{i'}$). The value of V_{max} decreased with increasing concentration of tested compound, while K_m slightly decreased. It means that **5p** binds reversibly to both free enzyme and enzyme-substrate complex. The result represents conformational changes of the *h*AChE and following changes in the active site. Corresponding K_i value of 3.28 ± 1.22 nM and $K_{i'}$ of 1.57 ± 0.28 nM were determined. Compound **5p** affects binding of substrate into the enzyme active site and interacts with peripheral active site (PAS) as well. This type of interaction plausibly broaden the profile of **5p** possessing Aβ anti-aggregating effect mediated through inhibition of *h*AChE PAS [48,49].

The same type of inhibition was revealed by donepezil that falls into category of dual-binding site AChEIs capable to counteract *h*AChE-accelerated Aβ aggregation (22 % at 100 μM) [50,51].

3.2.3. Determination of M1 mAChR activity

In order to explore whether novel tacrine-BQCA hybrids are able modulate the response mediated via M1 mAChR receptors, a calcium mobilization assay was used. Obtained activities were compared with BQCA, highly selective and effective positive allosteric modulator of M1 mAChRs (see Supporting Information) [21]. Unfortunately, from the whole series BQCA was the only one compound able to potentiate M1 mAChR–mediated calcium release. All newly prepared tacrine-BQCA hybrids exerted an antagonistic profile. Such discrepancy might be interpreted in light of preferential binding of different tacrine units into M1 mAChR allosteric site since such receptor-blocking interaction between tacrine itself and M1 mAChR has been previously demonstrated [52,53]. Not encouraged by the obtained data, the IC_{50} values demonstrating the antagonist effect of novel drug candidates were determined. All the hybrids displayed affinity towards M1 mAChR in the micromolar range highlighting **5i** as the most active antagonist (IC_{50}= 0.455 ± 0.061 μM) and **5f** as the least potent (IC_{50}= 11.4 ± 3.06 μM). Notably, the influence of the linker length on antagonistic effect was observed where compounds with 7-8 carbons in the linker exhibited the lowest inhibitory potency. Thus, the elongation of the spacer could lead to suppression of antagonistic effect towards M1 mAChRs [54]. Taken into account the potent AChE inhibition, AChE-selective profile and the lowest M1 mAChR antagonistic profile, **5f** can be highlighted and considered as worthy of further investigation.

3.2.4. Cytotoxicity evaluation

The main drawback disqualifying THA is coined with its severe hepatotoxicity [55]. THA administration is bound to liver function monitoring such as alanine aminotransferases (ALT) or lactate dehydrogenase (LDH) [56]. In this context, the scientific community eagerly searches for novel THA derivatives with reduced side effects linked to hepatotoxicity [26]. In this connection, we tested the potential *in vitro* hepatotoxic effect of nine selected compounds (selected pursuant to their IC_{50} values towards *h*AChE and *h*BChE) by measuring the HepG2 cell viability, using BQCA, tacrine, 6-Cl-THA and 7-MEOTA as standards (Table 2). Intriguingly, our results highlighted THA to be a the less toxic reference compound followed by 7-MEOTA, 6-Cl-THA and BQCA. *In vitro* toxicity of the agents may differ from *in vivo* toxicity due to the differences in pharmacokinetics and metabolism. Biotransformation processes potentially cause the toxicity [27]. All the tested tacrine-BQCA

heterodimers revealed one to two order of magnitude higher cytotoxic effect. This might be attributed to higher lipophilicity of compounds and molecular structure enlargement as observed previously in related studies [23,57]. On the contrary, highly lipophilic **5t** derivative bearing 6-Cl-THA scaffold proved to be the least toxic hybrid within the study with cytotoxicity higher than 40 μM. It is important to note that all the obtained data must be taken with a precaution as they do not reflect the real *in vivo* toxicity profile. For instance, it is well-known that during long-term clinical administration of THA its increased incidence of hepatotoxicity compared to 7-MEOTA was observed [26].

Table 2 HepG2 cell viability of selected tacrine-BQCA hybrids and reference compounds (n=3).

Compound	HepG2 IC_{50} ± SEM (μM)[a]
BQCA	> 40
THA	168.47 ± 3.91
7-MEOTA	44.37 ± 3.35
6-Cl-THA	43.20 ± 1.17
5a	1.63 ± 0.06
5b	2.42 ± 0.13
5f	0.60 ± 0.09
5h	1.44 ± 0.04
5i	2.17± 0.17
5l	2.72 ± 0.14
5o	3.48 ± 0.15
5p	4.99 ± 0.30
5t	> 40

[a] Means ± SEM of triplicates from three different measurements

3.2.5. In vitro BBB permeation assays

Parallel artificial membrane permeation assays (PAMPA) is a tool for predicting passive BBB permeation which is a fundamental parameter for drug acting in the CNS [58]. In this assay, the brain penetration of nine novel tacrine-BQCA hybrids was predicted. We optimized, the method due to limited compounds solubility. To improve the solubility of the compounds we used 1% solution of poloxamer pluronic F-127 validating the solubility data via the HPLC method (data not shown). However, the use of different solvents may affect the polar-brain-lipid (PBL) membrane. Indeed, it has been observed that the *P*e values of the reference compounds differ according the solvent used (phosphate buffer (PBS) or 1% F-127 in PBS) (Table S1 –Supplementary data). Even though, a clear correlation (Figure S2 – Supplementary data, R^2=0,9619) of *P*e values in both solvents could hardly be found in literature, the commonly reported thresholds for CNS available (*P*e > 4 x 10^{-6} cm s^{-1}) and for CNS unavailable (*P*e < 2 x 10^{-6} cm s^{-1}) in PBS may be shifted when using 1% F-127. Thus, we correlated the *P*e values obtained in the 1% F-127 for novel compounds with those obtained for standard

compounds, where CNS bioavailability is generally known. By a simple comparison of *P*e values we can estimate the probability of BBB penetration for novel compounds (Table 3).

The obtained data predicts that novel compounds from 7-MEOTA-BQCA subset, namely **5b** and **5f**, are able to cross the BBB via passive diffusion. Other derivatives fall into uncertain permeation interval or their BBB penetration is not probable at all (**5a** and **5h**). However, since our results indicated that lipid-mediated transport is uncertain, other mechanisms engaged in compounds delivery could be involved such as carrier-mediated, or receptor-mediated transports for large molecules that have a high affinity for an endogenous BBB receptor-mediated transport system [59].

Table 3 Prediction of the BBB permeation of novel compounds expressed as the *P*e value ± SEM (n = 3).

Compound	*P*e ± SEM (x 10^{-6} cm s^{-1}) 1% F-127	CNS [a]
5t	2.35 ± 0.25	+/-
5f	9.25 ± 1.80	+
5l	2.28 ± 0.58	+/-
5p	3.08 ± 0.07	+/-
5o	2.37 ± 0.47	+/-
5i	2.60 ± 0.61	+/-
5h	1.80 ± 0.10	-
5b	4.85 ± 0.05	+
5a	1.65 ± 0.25	-

[a] Prediction of BBB permeation is estimated for experimental conditions without F-127. CNS+ stands for the drugs in the CNS available, CNS- for unavailable and CNS+/- for the drugs with limited or uncertain access to the CNS.

3.3. Molecular modeling studies

To better investigate the structure-function relationships of tacrine-BQCA compounds at a molecular level, docking simulations were performed for the most potent compounds under the study into *h*AChE (PDB ID: 4EY7) and *h*BChE (PDB ID: 4BDS) active sites [60,61]. The characterization of **5f**-, **5i**- and **5p**-*h*AChE complexes were carried out, while **5a**, **5h** and **5o** were included to study ligand accommodation within *h*BChE active site.

Regarding *h*AChE, our results clearly delineate the obtained results from *in vitro* proposing that calculated binding affinities via AutoDock Vina 1.1.2 for **5f**, **5i** and **5p** were -14.4, - 15.3 and -16.7 kcal/mol, respectively. The orientation of **5f** (Fig. 3 A and B) in the *h*AChE active site placed the 7-MEOTA moiety outward the cavity gorge while BQCA scaffold was situated in the CAS region. In this case, Tyr72 (3.8 Å; cation-π interaction), Thr75, Tyr341 (2.2 and 2.7 Å, respectively; hydrogen bonds to methoxy-group from 7-MEOTA), Tyr124 (2.5 Å; hydrogen bond to exocyclic amino group),

Trp86 (3.5 Å; distorted parallel π-π interaction with 1,4-dihydroquinoline) are deemed to be crucial players for enzyme-ligand stability. Glu202 (3.2 Å) and Ser203 (3.3 Å) from catalytic triad showed favorable interactions by providing hydrogen bonds to ketone group from 1,4-dihydroquinoline. Consistency of our results is further emphasized by our previous findings where 7-MEOTA was shown to reside 180° rotated in relationship to THA [26]. This occupancy is less favorable yielding to lower AChE inhibitory potency. Indeed, the combination of 7-MEOTA with BQCA highlighted the latter moiety as more optimal CAS binder. On the contrary, **5i**-*h*AChE (Fig. 3 C and D) complex revealed opposite ligand anchoring with THA core placed proximally and BQCA moiety in distal direction. THA scaffold displayed parallel π-π/cation-π bonding with Trp86 (3.6 Å) in the CAS subsite. Interestingly, the catalytic triad residues remained unaffected. 1,4-Dihydroquinoline moiety is stacked against Tyr124 (4.3 Å; parallel π-π interaction). Importantly, Trp286 as a key PAS residue seems to have dual binding role when surrounding concomitantly 1,4-dihydroquinoline (4.1 Å) as well as 4-methoxybenzyl (4.3 Å) moieties. Completely different orientation can be found within **5p**-*h*AChE (Fig. 3 E and F) complex. Accordingly, 6-Cl-THA unit faces to Tyr337 (3.2 Å) by π-π stacking in parallel manner within CAS region. 1,4-Dihydroquinoline provide favorable stacking to Tyr341 (3.8 Å), while Tyr124 (4.0 Å) is engaged in anchoring 4-methoxybenzyl moiety of BQCA. Similarly, to **5i**-*h*AChE, **5p**-*h*AChE did not exert any interaction to catalytic triad residues. The importance of chlorine atom in 6-position of THA core is underlined by the presence of several halogen-alkyl/aryl interactions to Val340, Leu76, Trp439 and Tyr341. In general, the latter together with the different BQCA moiety lodging from **5f**- and **5i**-*h*AChE complexes can be denoted as the culprits for high affinity towards *h*AChE.

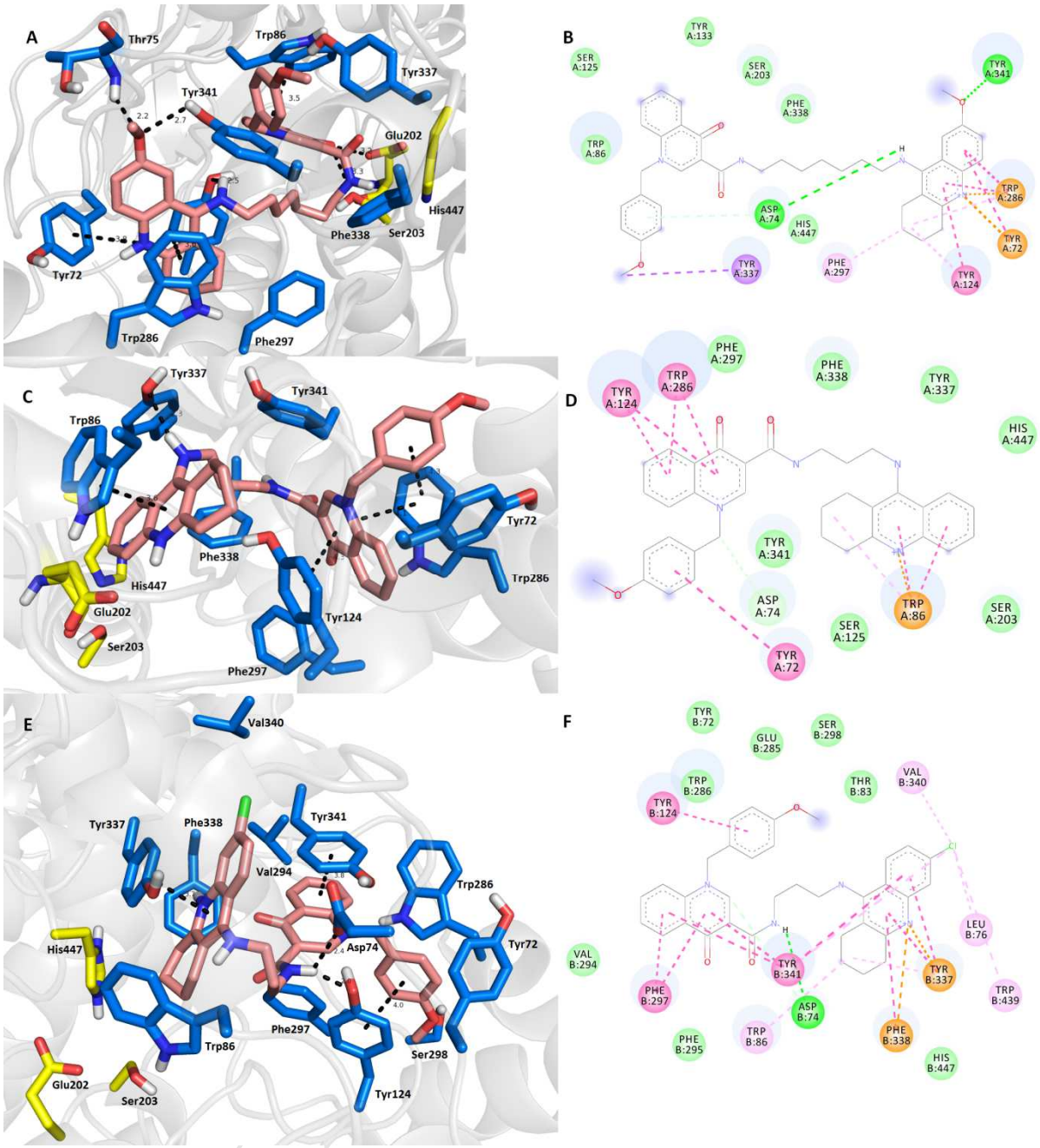

Figure 3. Docking results for the novel tacrine-BQCA hybrids (**5f**, **5i** and **5p**) within *h*AChE active site (PDB ID: 4EY7). A, C and E—Superimposed analogue **5f**, **5i** and **5p** (salmon carbon atoms) as 3D figures; B, D and F—2D representation of **5f**, **5i** and **5p**, respectively. Generally to (A, C, E)—important amino acid residues involved in the ligand-enzyme interactions are displayed as marine blue carbon atoms; catalytic triad residues (Glu202, Ser203, His447) are shown in yellow, rest of the enzyme is represented as light-grey cartoon. Figures (B, D and F) were created with Discovery Studio 2016 Client software; Figures (A, C and E) were generated with PyMol 1.5.0.4 (The PyMOL Molecular Graphics System, Version 1.5.0.4 Schrödinger, LLC, Mannheim, Germany).

From a structural point of view, BChE active site contains less aromatic residues within PAS region proposing that it can accommodate more bulkier substrates [62,63]. With this in mind, we have embedded the **5a**, **5h** and **5o** as the most active hybrids from each subset into the *h*BChE cavity highlighting several interesting findings. The scoring function clearly correlates well with the inhibition power from *in vitro* since the lowest binding energies calculated are as follows -13.3 kcal/mol, -14.0 kcal/mol and -13.4 kcal/mol for **5a**-, **5h**- and **5o**-*h*BChE complexes, respectively. Note that, we are aware of the fact that Autodock Vina software possesses comparatively low standard error of 2.85 kcal/mol which also has to be considered when docking the ligands [64,65]. **5a**-*h*BChE (Fig. 4 A and B) complex revealed manifold interactions with similar attributes as in **5f**-*h*AChE complex in terms of 7-MEOTA distal arrangement and proximal BQCA accommodation. Tyr332 (3.8 Å) is the major aromatic amino acid residue responsible for anchoring 7-MEOTA moiety of **5a**. BQCA moiety demonstrated several π-π interactions with Trp231 (1,4-dihydroquinoline moiety; 3.7 Å), Phe329 (1,4-dihydroquinoline moiety; 3.4 Å) and Trp82 (4-methoxybenzyl moiety; 3.7 Å). Some van der Waals forces can be found for catalytic triad residues, namely for His438 and Ser198. **5h** (Fig. 4 C and D) adapted very close spatial orientation as **5a** within *h*BChE active site. 6-Cl-THA preserved π-π stacking with Tyr332 (3.9 Å). In similar Trp231, Phe329 and Trp82 as well as van der Waals hydrophobic interacted with catalytic triad residues His438 and Ser198. Hydrogen bonds between Thr120 (2.4 Å) and oxygen from amidic function in combination with Gln119-ketone group from 1,4-dihydroquinoline (2.6 Å) are plausibly the key mediators responsible for higher affinity to *h*BChE compared to **5a** and **5o** complexes (see below). Generally, **5o** (Fig. 4 E and F) is likewise engaged in the same web of interactions as previously described **5a** and **5h** hybrids in the *h*BChE active site. Subtle differences can be seen such as missing π-π interaction to Trp231 and hydrogen bonds to Thr120 and Gln119. On the contrary, presence of chlorine atom at THA unit displayed favorable halogen-alkyl/aromatic interaction which somewhat counterbalance the latter mentioned missing interactions.

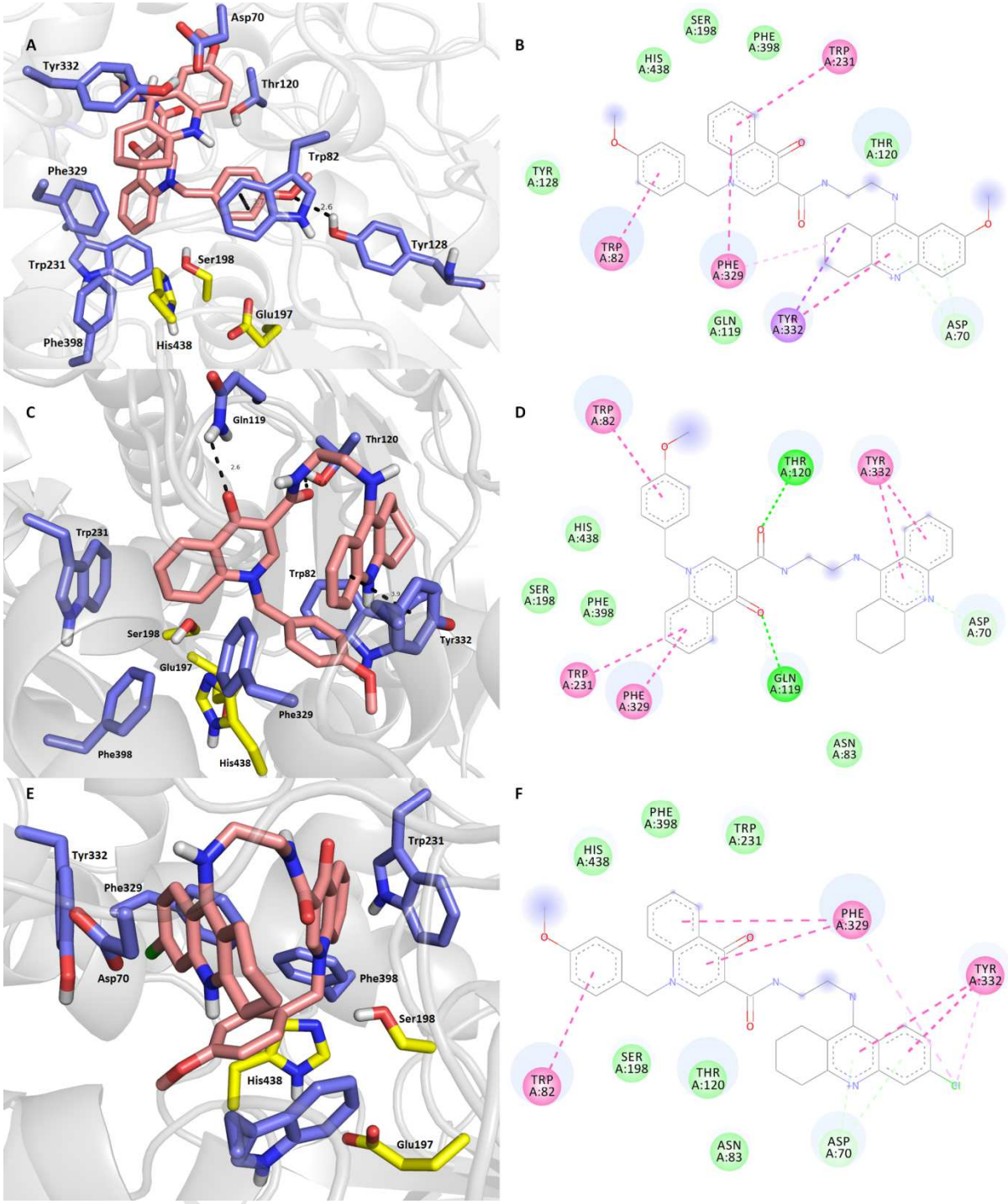

Figure 4. Docking results for the novel tacrine-BQCA hybrids (**5a**, **5h** and **5o**) within *h*BChE active site (PDB ID: 4BDS). A, C and E—Superimposed analogue **5a**, **5h** and **5o** (salmon carbon atoms) as 3D figures; B, D and F—2D representation of **5a**, **5h** and **5o**, respectively. Generally to (A, C, E)—important amino acid residues involved in the ligand-enzyme interactions are displayed as blue carbon atoms; catalytic triad residues (Glu197, Ser198, His438) are shown in yellow, rest of the enzyme is represented as light-grey cartoon. Figures (B, D and F) were created with Discovery Studio

2016 Client software; Figures (A, C and E) were generated with PyMol 1.5.0.4 (The PyMOL Molecular Graphics System, Version 1.5.0.4 Schrödinger, LLC, Mannheim, Germany).

4. CONCLUSION

In summary, we developed novel tacrine-BQCA hybrids presumably to counteract AD on double front following MTDL strategy i) indirectly by enhancing cholinergic transmission, i.e. by cholinesterase inhibition and ii) directly by supporting cholinergic transmission via M1 mAChR activation. However, the latter premise was not fulfilled since our concerns raised by preferential tacrine unit orientation into M1 mAChR which further exerted opposite (i.e. antagonistic) effect of the ligands. We believe that our findings do not rule out tacrine-BQCA from further testing. There is a need to test tacrine-BQCA potential from a broader perspective, for instance, under *in vivo* conditions where metabolism of the parent compound has to be taken into account. We can pinpoint compound **5o** possessing nanomolar, non-selective cholinesterase inhibition profile (*h*AChE IC_{50} = 74.5 nM; *h*BChE IC_{50} = 83.3 nM) with micromolar affinity towards M1 mAChR (IC_{50} = 4.23 μM). Non-selective pattern of cholinesterase inhibition is likely to be valuable during the onset as well as at later stages of AD.

5. EXPERIMENTAL PROTOCOL

5.1. Chemistry

All used chemical reagents were purchased from Sigma-Aldrich (Prague, Czech Republic). Solvents for synthesis were obtained from Penta chemicals Co. The course of the reactions was monitored by thin layer chromatography (TLC) on aluminium plates precoated with silica gel 60 F254 (Merck, Czech Republic) and then visualized by UV 254. Melting points were determined on a melting point apparatus M-565 (Büchi, Switzerland) and are uncorrected. NMR spectra of target compounds were recorded on Varian Mercury VX BB 300 (operating at 300 MHz for ^{1}H and 75 MHz for ^{13}C) or on Varian S500 spectrometer (operating at 500 MHz for ^{1}H and 126 MHz for ^{13}C; Varian Comp. Palo Alto, USA). Chemical shifts are reported in parts per million (ppm). Spin multiplicities are given as s (singlet), bs (broad singlet), d (doublet), dd (doublet of doublets), t (triplet), q (quartet), or m (multiplet). The coupling constants (*J*) are reported in Hertz (Hz). High-resolution mass spectra (HRMS) were determined by Q Exactive Plus hybrid quadrupole-orbitrap spectrometer.

BQCA synthesis followed previously published procedure [32]. Similarly, **4a**-**4u** intermediates were prepared according to the literature [23,40,66,67]. The spectroscopic data for all of these intermediates were in good agreement with the literature.

5.1.1. General procedure for synthesis of tacrine-BQCA Hybrids (5a-5u)

BQCA (0.5 mmol), and appropriate N^1-(1,2,3,4-tetrahydroacridin-9-yl)alkane-1,ω-diamine (**4a**-**4u**, 0.5 mmol) were dissolved in 5 mL of dry *N,N*-dimethylformamide (DMF) under argon atmosphere followed by addition of triethylamine (TEA; 1.5 mmol). Reaction was stirred for 1h, after that benzotriazol-1-yloxy)tris(dimethylamino)phosphonium hexafluorophosphate (BOP; 0.5 mmol) was added. Stirring continued for further 48h at RT. The reaction mixture was then extracted with water (100 mL) and ethyl-acetate (3 × 100 mL), dried with anhydrous sodium sulphate and solvent was removed *in vacuo*. The crude product was purified using column chromatography with chloroform-methanol as mobile phase (elution from 40:1 to 25:1; air pressured) to afford the tacrine-BQCA hybrids **5a**-**5u**.

5.1.1.1. N-{2-[(7-methoxy-1,2,3,4-tetrahydroacridin-9-yl)amino]ethyl}-1-[(4-methoxyphenyl)methyl]-4-oxo-1,4-dihydroquinoline-3-carboxamide (**5a**)

Intermediate **4a** and BQCA reacted according to the general procedure to give the desired product as brown solid (41 % yield): m.p. 128.4 – 130.1 °C; ^{1}H NMR (500 MHz, Acetone-d$_6$) δ 10.57 (t, *J* = 6.3 Hz, 1H), 9.01 (s, 1H), 8.43 (d, *J* = 8.1 Hz, 1H), 7.88 – 7.81 (m, 1H), 7.80 – 7.68 (m, 2H), 7.61 – 7.47 (m, 2H), 7.41 (d, *J* = 9.0 Hz, 1H), 7.29 (d, *J* = 8.2 Hz, 2H), 6.94 (d, *J* = 8.2 Hz, 2H), 5.70 (s, 2H), 4.20 (t, *J* = 5.1 Hz, 2H), 4.00 (s, 3H), 3.92 (t, *J* = 5.4 Hz, 2H), 3.77 (s, 3H), 3.07 – 2.96 (m, 2H), 2.96 – 2.88 (m, 2H), 1.99 – 1.83 (m, 4H); 13C NMR (126 MHz, Acetone-d$_6$) δ 176.92, 167.99, 160.60, 157.81, 155.65, 152.02, 149.26, 140.44, 136.23, 133.76, 129.17, 128.70, 127.97, 127.36, 125.97, 124.26, 123.70, 119.32, 118.60, 115.22, 113.82, 111.57, 103.91, 57.14, 56.35, 55.56, 51.39, 40.48, 30.29, 25.68, 23.08, 21.90; HRMS $[M+H]^+$: 563.2637 (calculated for: $[C_{34}H_{35}N_4O_4]^+$ 563.2614)

5.1.1.2. *N*-{3-[(7-methoxy-1,2,3,4-tetrahydroacridin-9-yl)amino]propyl}-1-[(4-methoxyphenyl)methyl]-4-oxo-1,4-dihydroquinoline-3-carboxamide (**5b**)

Intermediate **4b** and BQCA reacted according to the general procedure to give the desired product as yellow solid (78 % yield): m.p. 162.7-164.5 °C; ^{1}H NMR (500 MHz, Chloroform-*d*) δ 10.46 (t, *J* = 6.5 Hz, 1H), 8.86 (s, 1H), 8.49 (dd, *J* = 8.0, 1.5 Hz, 1H), 8.23 (d, *J* = 9.3 Hz, 1H), 7.69 – 7.64 (m, 1H), 7.63 (d, *J* = 2.6 Hz, 1H), 7.54 (d, *J* = 8.5 Hz, 1H), 7.51 – 7.45 (m, 1H), 7.29 (dd, *J* = 9.2, 2.4 Hz, 1H), 7.25 (t, *J* = 7.6 Hz, 1H), 7.15 – 7.11 (m, 2H), 6.90 – 6.85 (m, 2H), 5.48 (s, 2H), 3.94 – 3.91 (m, 5H), 3.77 (s, 3H), 3.70 – 3.65 (m, 2H), 3.19 (t, *J* = 6.1 Hz, 2H), 2.80 (t, *J* = 5.9 Hz, 2H), 2.04 – 1.97 (m, 2H), 1.92 – 1.82 (m, 4H); ^{13}C NMR (126 MHz, Chloroform-*d*) δ 176.76, 166.95, 159.72, 157.09, 155.27, 149.84, 148.03, 139.29, 133.14, 128.95, 128.14, 127.79, 127.02, 125.79, 125.21, 123.70, 121.94, 117.51, 117.04, 114.64, 111.28, 110.87, 102.82, 57.28, 55.81, 55.27, 43.32, 36.80, 35.38, 28.37, 24.75, 22.19, 21.39, 20.66; HRMS $[M+H]^+$: 577.2779 (calculated for: $[C_{35}H_{37}N_4O_4]^+$ 577.2770)

5.1.1.3. *N*-{4-[(7-methoxy-1,2,3,4-tetrahydroacridin-9-yl)amino]butyl}-1-[(4-methoxyphenyl)methyl]-4-oxo-1,4-dihydroquinoline-3-carboxamide (**5c**)

Intermediate **4c** and BQCA reacted according to the general procedure to give the desired product as yellow solid (91 % yield): m.p. 220.5-221.8 °C; ^{1}H NMR (300 MHz, Chloroform-*d*) δ 10.26 (t, *J* = 5.9 Hz, 1H), 8.78 (s, 1H), 8.40 (dd, *J* = 8.1, 1.5 Hz, 1H), 7.70 (dd, *J* = 9.3, 0.9 Hz, 1H), 7.67 – 7.60 (m, 1H), 7.53 – 7.39 (m, 4H), 7.07 (d, *J* = 8.5 Hz, 2H), 6.85 – 6.79 (m, 1H), 6.04 (bs, 1H), 5.39 (s, 2H), 4.03 – 3.94 (m, 2H), 3.86 (s, 3H), 3.74 (s, 3H), 3.59 – 3.49 (m, 2H), 2.98 – 2.90 (m, 2H), 2.65 – 2.58 (m, 2H), 2.03 – 1.75 (m, 8H); ^{13}C NMR (126 MHz, Chloroform-*d*) δ 176.64, 165.37, 159.64, 156.92, 155.46, 149.28, 147.92, 139.19, 133.07, 132.96, 127.77, 127.72, 126.79, 125.91, 125.28, 124.21, 121.09, 117.06, 116.93, 114.55, 111.43, 111.31, 103.61, 57.10, 55.81, 55.25, 47.67, 47.34, 38.47, 28.21, 28.14, 26.73, 23.67, 21.78, 20.49; HRMS $[M+H]^+$: 591.2942 (calculated for: $[C_{36}H_{39}N_4O_4]^+$ 591.2927)

5.1.1.4. *N*-{5-[(7-methoxy-1,2,3,4-tetrahydroacridin-9-yl)amino]pentyl}-1-[(4-methoxyphenyl)methyl]-4-oxo-1,4-dihydroquinoline-3-carboxamide (**5d**)

Intermediate **4d** and BQCA reacted according to the general procedure to give the desired product as yellow solid (58 % yield): m.p. 66.7-68.0 °C; ^{1}H NMR (300 MHz, Chloroform-*d*) δ 10.08 (t, *J* = 5.5 Hz, 1H), 8.86 (s, 1H), 8.47 (dd, *J* = 8.1, 1.6 Hz, 1H), 7.90 (d, *J* = 9.1 Hz, 1H), 7.60 (ddd, *J* = 8.6, 6.9, 1.6 Hz, 1H), 7.47 – 7.38 (m, 2H), 7.28 (d, *J* = 2.7 Hz, 1H), 7.21 (dd, *J* = 9.1, 2.7 Hz, 1H), 7.12 – 7.02 (m, 2H), 6.86 – 6.78 (m, 2H), 5.35 (s, 2H), 3.88 (s, 3H), 3.74 (s, 3H), 3.58 – 3.42 (m, 4H), 3.09 – 2.98 (m, 2H), 2.76 – 2.64 (m, 2H), 1.92 – 1.49 (m, 10H); ^{13}C NMR (75 MHz, Chloroform-*d*) δ 176.73, 164.96, 159.63, 156.06, 154.43, 151.10, 148.06, 139.18, 132.78, 127.98, 127.95, 127.65, 127.61, 127.03, 125.86, 125.06, 121.14, 120.17, 116.78, 115.67, 114.57, 111.85, 102.01, 57.15, 55.52, 55.23, 48.70, 38.75, 32.27, 31.16, 29.32, 24.51, 24.34, 22.71, 22.18; HRMS $[M+H]^+$: 605.3085 (calculated for: $[C_{37}H_{41}N_4O_4]^+$ 605.3083

5.1.1.5. *N*-{6-[(7-methoxy-1,2,3,4-tetrahydroacridin-9-yl)amino]hexyl}-1-[(4-methoxyphenyl)methyl]-4-oxo-1,4-dihydroquinoline-3-carboxamide (**5e**)

Intermediate **4e** and BQCA reacted according to the general procedure to give the desired product as brown solid (37 % yield): m.p. 76.7-78.7 °C; ^{1}H NMR (300 MHz, Chloroform-*d*) δ 10.03 (t, *J* = 5.8 Hz, 1H), 8.79 (s, 1H), 8.37 (dd, *J* = 8.1, 1.5 Hz, 1H), 7.78 (d, *J* = 9.1 Hz, 1H), 7.60 – 7.50 (m, 1H), 7.45 – 7.28 (m, 2H), 7.24 – 7.14 (m, 1H), 7.05 – 6.97 (m, 2H), 6.80 – 6.70 (m, 2H), 5.31 (s, 2H), 3.81 (s, 3H), 3.66 (s, 2H), 3.45 – 3.34 (m, 2H), 3.02 – 2.90 (m, 2H), 2.65 – 2.51 (m, 2H), 1.91 – 1.12 (m, 14H).; ^{13}C NMR (75 MHz, Chloroform-*d*) δ 176.79, 165.08, 159.94, 159.67, 156.75, 156.64, 148.84, 148.06, 139.25, 134.09, 132.93, 127.94, 127.75, 126.99, 125.94, 125.17, 123.08, 117.48, 116.93, 114.81, 114.60,

111.79, 103.02, 57.16, 55.78, 55.28, 47.97, 38.70, 31.00, 29.68, 29.36, 26.32, 26.03, 24.06, 22.20, 21.22; HRMS $[M+H]^+$: 619.3253 (calculated for: $[C_{38}H_{43}N_4O_4]^+$ 619.3240

5.1.1.6. *N*-{7-[(7-methoxy-1,2,3,4-tetrahydroacridin-9-yl)amino]heptyl}-1-[(4-methoxyphenyl)methyl]-4-oxo-1,4-dihydroquinoline-3-carboxamide (**5f**)

Intermediate **4f** and BQCA reacted according to the general procedure to give the desired product as brown solid (53 % yield): m.p. 90.8-92.8 °C; ^{1}H NMR (500 MHz, Chloroform-*d*) δ 10.06 (t, *J* = 5.6 Hz, 1H), 8.89 (s, 1H), 8.48 (dd, *J* = 8.1, 1.6 Hz, 1H), 7.86 (d, *J* = 9.2 Hz, 1H), 7.60 (ddd, *J* = 8.6, 7.0, 1.6 Hz, 1H), 7.48 – 7.38 (m, 2H), 7.29 (d, *J* = 2.7 Hz, 1H), 7.23 (dd, *J* = 9.2, 2.7 Hz, 1H), 7.08 (d, *J* = 8.7 Hz, 2H), 6.85 – 6.81 (m, 2H), 5.37 (s, 2H), 3.90 (s, 3H), 3.75 (s, 3H), 3.54 (t, *J* = 7.2 Hz, 2H), 3.46 (td, *J* = 6.9, 5.6 Hz, 2H), 3.06 – 2.99 (m, 2H), 2.72 – 2.66 (m, 2H), 1.88 (p, *J* = 4.5 Hz, 4H), 1.76 – 1.60 (m, 4H), 1.49 – 1.37 (m, 6H); ^{13}C NMR (126 MHz, Chloroform-*d*) δ 176.74, 164.84, 159.63, 156.09, 154.05, 151.44, 148.07, 148.06, 139.19, 132.73, 127.96, 127.62, 127.44, 127.02, 125.91, 125.00, 121.38, 119.95, 116.76, 115.35, 114.56, 111.94, 102.16, 57.12, 55.52, 55.23, 48.78, 39.05, 32.01, 31.42, 29.38, 28.90, 26.85, 26.70, 24.35, 22.63, 22.10; HRMS $[M+H]^+$: 633.3401 (calculated for: $[C_{39}H_{45}N_4O_4]^+$ 633.3396

5.1.1.7. *N*-{8-[(7-methoxy-1,2,3,4-tetrahydroacridin-9-yl)amino]octyl}-1-[(4-methoxyphenyl)methyl]-4-oxo-1,4-dihydroquinoline-3-carboxamide (**5g**)

Intermediate **4g** and BQCA reacted according to the general procedure to give the desired product as brown solid (26 % yield): m.p. 76.7-78.0 °C; ^{1}H NMR (300 MHz, Chloroform-*d*) δ 10.07 (t, *J* = 5.6 Hz, 1H), 8.87 (s, 1H), 8.44 (dd, *J* = 8.1, 1.6 Hz, 1H), 7.81 (d, *J* = 9.3 Hz, 1H), 7.65 – 7.55 (m, 1H), 7.46 (d, *J* = 8.6 Hz, 1H), 7.43 – 7.36 (m, 2H), 7.32 – 7.26 (m, 1H), 7.13 – 7.02 (m, 2H), 6.87 – 6.76 (m, 2H), 5.37 (s,2H), 3.88 (s, 3H), 3.83 – 3.74 (m, 2H), 3.73 (s, 3H), 3.51 – 3.34 (m, 2H), 3.05 – 2.95 (m, 2H), 1.99 – 1.51 (m, 8H), 1.49 – 1.18 (m, 10H); ^{13}C NMR (75 MHz, Chloroform-*d*) δ 176.74, 164.91, 159.59, 156.62, 154.14, 150.73, 148.05, 139.20, 135.57, 132.84, 127.89, 127.67, 126.91, 125.92, 125.07, 123.30, 123.19, 117.95, 116.88, 114.53, 112.62, 111.80, 103.19, 57.11, 55.69, 55.22, 48.33, 39.10, 36.79, 36.73, 31.00, 29.43, 28.89, 26.75, 26.48, 23.79, 22.05, 21.08; HRMS $[M+H]^+$: 647.3577 (calculated for: $[C_{40}H_{47}N_4O_4]^+$ 647.3553

5.1.1.8. 1-[(4-methoxyphenyl)methyl]-4-oxo-*N*-{2-[(1,2,3,4-tetrahydroacridin-9-yl)amino]ethyl}-1,4-dihydroquinoline-3-carboxamide (**5h**)

Intermediate **4h** and BQCA reacted according to the general procedure to give the desired product as brown solid (63 % yield): m.p. 125.0-126.3 °C; ^{1}H NMR (500 MHz, Chloroform-*d*) δ 10.44 (t, *J* = 5.3 Hz, 1H), 8.91 (s, 1H), 8.50 (dd, *J* = 8.1, 1.6 Hz, 1H), 8.07 (dd, *J* = 8.6, 1.3 Hz, 1H), 7.92 (dd, *J* = 8.5, 1.2 Hz, 1H), 7.61 (ddd, *J* = 8.6, 7.0, 1.7 Hz, 1H), 7.52 (ddd, *J* = 8.3, 6.8, 1.3 Hz, 1H), 7.47 – 7.42 (m, 2H), 7.31 (ddd, *J* = 8.3, 6.8, 1.3 Hz, 1H), 7.11 – 7.06 (m, 2H), 6.87 – 6.83 (m, 2H), 5.39 (s, 2H), 3.83 – 3.77 (m,

4H), 3.76 (s, 3H), 3.04 (t, *J* = 6.0 Hz, 2H), 2.77 (t, *J* = 5.9 Hz, 2H), 1.93 – 1.82 (m, 4H); ^{13}C NMR (126 MHz, Chloroform-*d*) *δ* 176.72, 166.52, 159.78, 157.87, 151.17, 148.20, 146.58, 139.28, 132.95, 128.49, 128.02, 127.67, 127.24, 125.87, 125.29, 123.72, 122.94, 119.82, 116.84, 115.68, 114.70, 114.05, 111.45, 57.25, 55.31, 50.33, 40.28, 33.54, 25.08, 23.05, 22.61; HRMS $[M+H]^+$: 533.2549 (calculated for: $[C_{33}H_{33}N_4O_3]^+$ 533.2508

5.1.1.9. 1-[(4-methoxyphenyl)methyl]-4-oxo-*N*-{3-[(1,2,3,4-tetrahydroacridin-9-yl)amino]propyl}-1,4-dihydroquinoline-3-carboxamide (**5i**)

Intermediate **4i** and BQCA reacted according to the general procedure to give the desired product as brown solid (23 % yield): m.p. 148.1-150.7 °C; ^{1}H NMR (500 MHz, Chloroform-*d*) *δ* 10.31 (t, *J* = 6.3 Hz, 1H), 8.91 (s, 1H), 8.51 (dd, *J* = 8.1, 1.6 Hz, 1H), 8.16 – 8.10 (m, 2H), 7.63 (ddd, *J* = 8.7, 7.0, 1.6 Hz, 1H), 7.56 (ddd, *J* = 8.3, 6.8, 1.3 Hz, 1H), 7.51 – 7.43 (m, 2H), 7.37 (ddd, *J* = 8.3, 6.8, 1.3 Hz, 1H), 7.14 – 7.08 (m, 2H), 6.89 – 6.84 (m, 2H), 5.44 (s, 2H), 3.76 (s, 3H), 3.72 (t, *J* = 6.2 Hz, 2H), 3.68 – 3.63 (m, 2H), 3.17 – 3.12 (m, 2H), 2.81 – 2.75 (m, 2H), 2.00 – 1.93 (m, 2H), 1.88 (m, 4H); ^{13}C NMR (126 MHz, Chloroform-*d*) *δ* 176.77, 166.18, 159.72, 155.54, 152.75, 148.14, 139.24, 132.95, 129.71, 127.95, 127.64, 127.12, 125.77, 125.44, 125.27, 124.21, 123.01, 118.45, 116.86, 114.65, 114.14, 111.34, 57.29, 55.26, 44.77, 35.88, 31.57, 29.61, 24.71, 22.67, 21.89; HRMS $[M+H]^+$: 547.2670 (calculated for: $[C_{34}H_{35}N_4O_3]^+$ 547.2664

5.1.1.10. 1-[(4-methoxyphenyl)methyl]-4-oxo-*N*-{4-[(1,2,3,4-tetrahydroacridin-9-yl)amino]butyl}-1,4-dihydroquinoline-3-carboxamide (**5j**)

Intermediate **4j** and BQCA reacted according to the general procedure to give the desired product as yellow amorphous solid (19 % yield): ^{1}H NMR (500 MHz, Chloroform-*d*) *δ* 10.16 (t, *J* = 5.8 Hz, 1H), 8.88 (s, 1H), 8.51 (dd, *J* = 8.2, 1.6 Hz, 1H), 8.00 (dd, *J* = 8.6, 1.3 Hz, 1H), 7.93 (dd, *J* = 8.4, 1.2 Hz, 1H), 7.63 (ddd, *J* = 8.6, 7.0, 1.7 Hz, 1H), 7.53 (ddd, *J* = 8.3, 6.8, 1.3 Hz, 1H), 7.50 – 7.42 (m, 2H), 7.34 (ddd, *J* = 8.3, 6.8, 1.3 Hz, 1H), 7.13 – 7.08 (m, 2H), 6.88 – 6.83 (m, 2H), 5.40 (s, 2H), 3.77 (s, 3H), 3.61 (t, *J* = 6.8 Hz, 2H), 3.57 – 3.51 (m, 2H), 3.10 – 3.03 (m, 2H), 2.74 – 2.67 (m, 2H), 1.88 – 1.76 (m, 4H), 1.28 – 1.22 (m, 4H); ^{13}C NMR (126 MHz, Chloroform-*d*) *δ* 176.78, 165.04, 159.71, 157.37, 151.31, 148.09, 146.12, 139.25, 132.81, 128.79, 128.01, 127.65, 127.46, 127.13, 125.88, 125.11, 123.84, 123.00, 119.58, 116.79, 115.32, 114.64, 111.86, 57.22, 55.26, 48.96, 38.73, 33.17, 29.64, 29.63, 29.14, 27.09, 24.59, 22.83, 22.42; HRMS $[M+H]^+$: 561.2853 (calculated for: $[C_{35}H_{37}N_4O_3]^+$ 561.2821

5.1.1.11. 1-[(4-methoxyphenyl)methyl]-4-oxo-*N*-{5-[(1,2,3,4-tetrahydroacridin-9-yl)amino]pentyl}-1,4-dihydroquinoline-3-carboxamide (**5k**)

Intermediate **4k** and BQCA reacted according to the general procedure to give the desired product as yellow amorphous solid (25 % yield): ^{1}H NMR (500 MHz, Chloroform-*d*) *δ* 10.18 (t, *J* = 5.8 Hz, 1H),

8.83 (s, 1H), 8.41 (dd, *J* = 8.1, 1.6 Hz, 1H), 8.19 (d, *J* = 8.7 Hz, 1H), 7.83 (d, *J* = 8.5 Hz, 1H), 7.67 – 7.58 (m, 2H), 7.50 (d, *J* = 8.7 Hz, 1H), 7.46 – 7.39 (m, 2H), 7.10 – 7.05 (m, 2H), 6.83 – 6.78 (m, 2H), 5.38 (s, 2H), 3.97 – 3.87 (m, 2H), 3.73 (s, 3H), 3.55 – 3.40 (m, 2H), 2.95 (t, *J* = 6.3 Hz, 2H), 2.56 (t, *J* = 6.2 Hz, 2H), 1.95 – 1.87 (m, 2H), 1.87 – 1.75 (m, 4H), 1.75 – 1.68 (m, 2H), 1.62 – 1.54 (m, 2H); ^{13}C NMR (126 MHz, Chloroform-*d*) *δ* 176.70, 165.20, 159.63, 156.14, 150.44, 148.04, 139.20, 138.24, 133.02, 133.00, 127.79, 127.73, 126.82, 125.93, 125.33, 125.22, 124.83, 119.74, 117.04, 115.44, 114.55, 111.55, 111.28, 57.12, 55.25, 48.50, 38.64, 30.06, 29.64, 28.96, 28.21, 23.91, 21.60, 20.48; HRMS $[M+H]^+$: 575.2985 (calculated for: $[C_{36}H_{39}N_4O_3]^+$ 575.2977

5.1.1.12. 1-[(4-methoxyphenyl)methyl]-4-oxo-*N*-{6-[(1,2,3,4-tetrahydroacridin-9-yl)amino]hexyl}-1,4-dihydroquinoline-3-carboxamide (**5l**)

Intermediate **4l** and BQCA reacted according to the general procedure to give the desired product as brown solid (60 % yield): m.p. 54.2-56.2 °C; ^{1}H NMR (500 MHz, Chloroform-*d*) *δ* 10.07 (t, *J* = 5.7 Hz, 1H), 8.88 (s, 1H), 8.49 (dd, *J* = 8.1, 1.6 Hz, 1H), 8.01 – 7.93 (m, 2H), 7.60 (ddd, *J* = 8.6, 7.0, 1.6 Hz, 1H), 7.53 (ddd, *J* = 8.4, 6.8, 1.4 Hz, 1H), 7.46 – 7.40 (m, 2H), 7.33 (ddd, *J* = 8.3, 6.8, 1.3 Hz, 1H), 7.11 – 7.05 (m, 2H), 6.87 – 6.81 (m, 2H), 5.35 (s, 2H), 3.75 (s, 3H), 3.53 (t, *J* = 7.2 Hz, 2H), 3.48 (td, *J* = 6.9, 5.7 Hz, 2H), 3.09 – 3.04 (m, 2H), 2.72 – 2.65 (m, 2H), 1.94 – 1.86 (m, 4H), 1.75 – 1.63 (m, 4H), 1.54 – 1.43 (m, 4H); ^{13}C NMR (126 MHz, Chloroform-*d*) *δ* 176.75, 164.85, 159.64, 157.49, 151.20, 148.06, 146.33, 139.19, 132.69, 128.62, 127.99, 127.69, 127.60, 127.08, 125.89, 124.99, 123.67, 122.94, 119.61, 116.70, 115.15, 114.57, 111.97, 57.12, 55.22, 49.17, 38.90, 33.30, 31.46, 29.41, 26.69, 26.47, 24.57, 22.83, 22.45; HRMS $[M+H]^+$: 589.3156 (calculated for: $[C_{37}H_{41}N_4O_3]^+$ 589.3134

5.1.1.13. 1-[(4-methoxyphenyl)methyl]-4-oxo-*N*-{7-[(1,2,3,4-tetrahydroacridin-9-yl)amino]heptyl}-1,4-dihydroquinoline-3-carboxamide (**5m**)

Intermediate **4m** and BQCA reacted according to the general procedure to give the desired product as brown amorphous solid (55 % yield): ^{1}H NMR (500 MHz, Chloroform-*d*) *δ* 10.06 (t, *J* = 5.7 Hz, 1H), 8.90 (s, 1H), 8.50 (dd, *J* = 8.1, 1.6 Hz, 1H), 7.99 (dd, *J* = 8.5, 1.3 Hz, 1H), 7.92 (dd, *J* = 8.5, 1.3 Hz, 1H), 7.60 (ddd, *J* = 8.6, 7.0, 1.7 Hz, 1H), 7.54 (ddd, *J* = 8.4, 6.8, 1.3 Hz, 1H), 7.47 – 7.40 (m, 2H), 7.34 (ddd, *J* = 8.4, 6.8, 1.3 Hz, 1H), 7.11 – 7.06 (m, 2H), 6.87 – 6.81 (m, 2H), 5.36 (s, 2H), 3.75 (s, 3H), 3.57 – 3.51 (m, 2H), 3.51 – 3.45 (m, 2H), 3.08 – 3.03 (m, 2H), 2.71 – 2.66 (m, 2H), 1.93 – 1.86 (m, 4H), 1.74 – 1.62 (m, 4H), 1.49 – 1.38 (m, 6H); ^{13}C NMR (126 MHz, Chloroform-*d*) *δ* 176.76, 164.83, 159.64, 157.25, 151.43, 148.09, 146.14, 139.21, 132.69, 128.79, 128.01, 127.61, 127.38, 127.08, 125.92, 124.98, 123.72, 123.08, 119.49, 116.72, 115.05, 114.58, 112.01, 57.12, 55.22, 49.29, 39.07, 33.14, 31.48, 29.61, 29.42, 28.91, 26.86, 26.69, 24.49, 22.79, 22.41; HRMS $[M+H]^+$: 603.3291 (calculated for: $[C_{38}H_{43}N_4O_3]^+$ 603.3290

5.1.1.14. 1-[(4-methoxyphenyl)methyl]-4-oxo-*N*-{8-[(1,2,3,4-tetrahydroacridin-9-yl)amino]octyl}-1,4-dihydroquinoline-3-carboxamide (**5n**)

Intermediate **4n** and BQCA reacted according to the general procedure to give the desired product as yellow amorphous solid (30 % yield): ^{1}H NMR (500 MHz, Chloroform-*d*) δ 10.08 – 10.01 (m, 1H), 8.89 (t, *J* = 2.3 Hz, 1H), 8.51 – 8.44 (m, 1H), 8.19 – 8.04 (m, 2H), 7.64 – 7.55 (m, 2H), 7.49 – 7.33 (m, 2H), 7.13 – 7.05 (m, 2H), 6.88 – 6.80 (m, 2H), 5.38 (s, 2H), 3.75 (s, 3H), 3.73 – 3.65 (m, 2H), 3.51 – 3.42 (m, 2H), 3.18 – 3.11 (m, 2H), 2.67 – 2.60 (m, 2H), 1.94 – 1.83 (m, 4H), 1.79 – 1.69 (m, 2H), 1.69 – 1.57 (m, 2H), 1.49 – 1.30 (m, 8H); ^{13}C NMR (126 MHz, Chloroform-*d*) δ 176.76, 164.82, 159.66, 153.10, 148.08, 139.21, 139.18, 132.72, 130.25, 127.99, 127.63, 127.04, 125.91, 125.00, 124.69, 124.28, 123.52, 117.88, 116.76, 114.58, 113.98, 112.01, 109.92, 57.15, 55.24, 53.37, 49.00, 39.08, 33.74, 31.84, 31.35, 31.28, 30.11, 29.61, 29.45, 29.27, 29.07, 28.96, 26.80, 26.60, 24.06, 22.61, 22.39, 21.64; HRMS $[M+H]^+$: 617.3458 (calculated for: $[C_{39}H_{45}N_4O_3]^+$ 617.3447

5.1.1.15. *N*-{2-[(6-chloro-1,2,3,4-tetrahydroacridin-9-yl)amino]ethyl}-1-[(4-methoxyphenyl)methyl]-4-oxo-1,4-dihydroquinoline-3-carboxamide (**5o**)

Intermediate **4o** and BQCA reacted according to the general procedure to give the desired product as brown solid (31 % yield): m.p. 162.5-164.0 °C; ^{1}H NMR (500 MHz, Chloroform-*d*) δ 10.51 – 10.42 (m, 1H), 8.91 (s, 1H), 8.50 (dd, *J* = 8.1, 1.5 Hz, 1H), 8.02 (d, *J* = 9.1 Hz, 1H), 7.89 (d, *J* = 2.2 Hz, 1H), 7.64 (ddd, *J* = 8.7, 7.0, 1.6 Hz, 1H), 7.51 – 7.43 (m, 2H), 7.24 (dd, *J* = 9.1, 2.2 Hz, 1H), 7.15 – 7.08 (m, 2H), 6.91 – 6.85 (m, 2H), 5.42 (s, 2H), 3.83 – 3.78 (m, 4H), 3.78 (s, 3H), 3.02 (t, *J* = 5.9 Hz, 2H), 2.79 – 2.73 (m, 2H), 1.92 – 1.83 (m, 4H); ^{13}C NMR (126 MHz, Chloroform-*d*) δ 176.68, 166.66, 159.77, 158.97, 151.23, 148.11, 139.25, 134.17, 132.96, 127.97, 127.63, 127.22, 126.70, 125.73, 125.32, 124.53, 124.27, 117.98, 116.79, 115.53, 114.70, 111.29, 57.27, 55.28, 40.21, 36.81, 36.78, 25.02, 22.91, 22.45; HRMS $[M+H]^+$: 567.2146 (calculated for: $[C_{33}H_{32}ClN_4O_3]^+$ 567.2118

5.1.1.16. *N*-{3-[(6-chloro-1,2,3,4-tetrahydroacridin-9-yl)amino]propyl}-1-[(4-methoxyphenyl)methyl]-4-oxo-1,4-dihydroquinoline-3-carboxamide (**5p**)

Intermediate **4p** and BQCA reacted according to the general procedure to give the desired product as brown solid (39 % yield): m.p. 95.4-96.1 °C; ^{1}H NMR (500 MHz, Chloroform-*d*) δ 10.26 (t, *J* = 6.3 Hz, 1H), 8.92 (s, 1H), 8.51 (dd, *J* = 8.0, 1.6 Hz, 1H), 8.03 (d, *J* = 9.1 Hz, 1H), 7.90 (d, *J* = 2.2 Hz, 1H), 7.63 (ddd, *J* = 8.6, 7.0, 1.6 Hz, 1H), 7.50 – 7.43 (m, 2H), 7.29 – 7.22 (m, 1H), 7.14 – 7.07 (m, 2H), 6.91 – 6.82 (m, 2H), 5.43 (s, 2H), 3.77 (s, 3H), 3.67 – 3.55 (m, 4H), 3.03 (t, *J* = 6.2 Hz, 2H), 2.75 (t, *J* = 5.2 Hz, 2H), 1.95 – 1.84 (m, 6H); ^{13}C NMR (126 MHz, Chloroform-*d*) δ 176.78, 165.93, 159.73, 151.21, 148.14, 139.25, 134.24, 132.91, 127.98, 127.79, 127.63, 127.15, 126.60, 125.79, 125.24, 124.45, 124.40,

118.15, 116.80, 115.77, 114.82, 114.66, 111.50, 57.27, 55.26, 45.19, 36.79, 36.76, 35.97, 31.58, 29.62, 24.97, 22.87, 22.43; HRMS $[M+H]^+$: 581.2294 (calculated for: $[C_{34}H_{34}ClN_4O_3]^+$ 581.2275

5.1.1.17. *N*-{4-[(6-chloro-1,2,3,4-tetrahydroacridin-9-yl)amino]butyl}-1-[(4-methoxyphenyl)methyl]-4-oxo-1,4-dihydroquinoline-3-carboxamide (**5q**)

Intermediate **4q** and BQCA reacted according to the general procedure to give the desired product as yellow pale solid (45 % yield): m.p. 65.3-66.7 °C; ^{1}H NMR (500 MHz, Chloroform-*d*) δ 10.15 (t, *J* = 5.8 Hz, 1H), 8.88 (s, 1H), 8.50 (dd, *J* = 8.1, 1.6 Hz, 1H), 7.91 (d, *J* = 9.1 Hz, 1H), 7.85 (d, *J* = 2.2 Hz, 1H), 7.62 (ddd, *J* = 8.6, 7.0, 1.6 Hz, 1H), 7.49 – 7.42 (m, 2H), 7.24 (dd, *J* = 9.1, 2.2 Hz, 1H), 7.12 – 7.07 (m, 2H), 6.88 – 6.83 (m, 2H), 5.39 (s, 2H), 3.76 (s, 3H), 3.59 – 3.50 (m, 4H), 3.03 – 2.98 (m, 2H), 2.70 – 2.66 (m, 2H), 1.92 – 1.86 (m, 4H), 1.85 – 1.74 (m, 4H); ^{13}C NMR (126 MHz, Chloroform-*d*) δ 176.75, 165.02, 159.69, 159.21, 150.75, 148.06, 147.73, 139.21, 133.97, 132.79, 127.98, 127.63, 127.18, 127.10, 125.85, 125.11, 124.57, 124.23, 118.25, 116.75, 115.73, 114.62, 111.82, 57.20, 55.24, 49.08, 38.69, 33.79, 29.20, 27.04, 24.55, 22.82, 22.50; HRMS $[M+H]^+$: 595.2447 (calculated for: $[C_{35}H_{36}ClN_4O_3]^+$ 595.2431

5.1.1.18. *N*-{5-[(6-chloro-1,2,3,4-tetrahydroacridin-9-yl)amino]pentyl}-1-[(4-methoxyphenyl)methyl]-4-oxo-1,4-dihydroquinoline-3-carboxamide (**5r**)

Intermediate **4r** and BQCA reacted according to the general procedure to give the desired product as brown amorphous solid (52 % yield): ^{1}H NMR (500 MHz, Chloroform-*d*) δ 10.11 (t, *J* = 5.8 Hz, 1H), 8.89 (s, 1H), 8.53 – 8.48 (m, 1H), 7.96 – 7.91 (m, 2H), 7.62 (ddd, *J* = 8.6, 7.0, 1.6 Hz, 1H), 7.49 – 7.43 (m, 2H), 7.27 – 7.24 (m, 1H), 7.11 – 7.06 (m, 2H), 6.88 – 6.82 (m, 2H), 5.39 (s, 2H), 3.77 (s, 3H), 3.62 – 3.44 (m, 4H), 3.06 – 3.01 (m, 2H), 2.68 – 2.65 (m, 2H), 1.93 – 1.84 (m, 4H), 1.81 – 1.68 (m, 4H), 1.61 – 1.52 (m, 2H); ^{13}C NMR (126 MHz, Chloroform-*d*) δ 176.80, 165.00, 159.72, 151.22, 148.11, 139.24, 139.22, 132.80, 128.02, 127.64, 127.14, 125.87, 125.10, 124.69, 124.38, 116.77, 114.64, 114.01, 111.94, 57.22, 55.27, 49.27, 38.76, 36.82, 36.78, 31.22, 29.64, 29.61, 29.31, 29.28, 24.48, 24.29, 22.75, 22.35; HRMS $[M+H]^+$: 609.2593 (calculated for: $[C_{36}H_{38}ClN_4O_3]^+$ 609.2588

5.1.1.19. *N*-{6-[(6-chloro-1,2,3,4-tetrahydroacridin-9-yl)amino]hexyl}-1-[(4-methoxyphenyl)methyl]-4-oxo-1,4-dihydroquinoline-3-carboxamide (**5s**)

Intermediate **4s** and BQCA reacted according to the general procedure to give the desired product as yellow amorphous solid (80 % yield): ^{1}H NMR (500 MHz, Chloroform-*d*) δ 10.06 (t, *J* = 5.7 Hz, 1H), 8.88 (s, 1H), 8.48 (dd, *J* = 8.1, 1.7 Hz, 1H), 7.90 (d, *J* = 9.0 Hz, 1H), 7.86 (d, *J* = 2.2 Hz, 1H), 7.60 (ddd, *J* = 8.6, 7.0, 1.7 Hz, 1H), 7.47 – 7.39 (m, 2H), 7.23 (dd, *J* = 9.0, 2.2 Hz, 1H), 7.10 – 7.05 (m, 2H), 6.86 – 6.80 (m, 2H), 5.36 (s, 2H), 3.75 (s, 3H), 3.52 – 3.45 (m, 4H), 3.03 – 2.98 (m, 2H), 2.68-2.64 (m, 2H), 1.92 – 1.86 (m, 4H), 1.73 – 1.63 (m, 4H), 1.52 – 1.43 (m, 4H); ^{13}C NMR (126 MHz, Chloroform-*d*) δ 176.75,

164.85, 159.65, 159.04, 150.91, 148.06, 147.64, 139.19, 134.01, 132.71, 127.98, 127.60, 127.07, 125.88, 125.01, 124.62, 124.15, 118.12, 116.70, 115.43, 114.58, 111.97, 57.13, 55.22, 49.29, 38.87, 36.78, 33.71, 29.37, 26.65, 26.43, 24.47, 22.79, 22.47; HRMS $[M+H]^+$: 623.2768 (calculated for: $[C_{37}H_{40}ClN_4O_3]^+$ 623.2744

5.1.1.20. *N*-{7-[(6-chloro-1,2,3,4-tetrahydroacridin-9-yl)amino]heptyl}-1-[(4-methoxyphenyl)methyl]-4-oxo-1,4-dihydroquinoline-3-carboxamide (**5t**)

Intermediate **4t** and BQCA reacted according to the general procedure to give the desired product as yellow pale solid (40 % yield): m.p. 82.0-84.7 °C; ^{1}H NMR (500 MHz, Chloroform-*d*) δ 10.04 (t, *J* = 5.7 Hz, 1H), 8.89 (s, 1H), 8.49 (dd, *J* = 8.1, 1.6 Hz, 1H), 7.93 – 7.86 (m, 2H), 7.60 (ddd, *J* = 8.6, 7.0, 1.6 Hz, 1H), 7.47 – 7.39 (m, 2H), 7.24 (dd, *J* = 9.0, 2.2 Hz, 1H), 7.13 – 7.04 (m, 2H), 6.87 – 6.80 (m, 2H), 5.37 (s, 2H), 3.75 (s, 3H), 3.52 – 3.43 (m, 4H), 3.04 – 2.98 (m, 2H), 2.66 – 2.64 (m, 2H), 1.94 – 1.85 (m, 4H), 1.73 – 1.60 (m, 4H), 1.51 – 1.37 (m, 6H); ^{13}C NMR (126 MHz, Chloroform-*d*) δ 176.83, 164.88, 159.71, 159.16, 150.98, 148.15, 147.78, 139.27, 134.07, 132.76, 128.07, 127.66, 127.21, 127.15, 125.96, 125.05, 124.68, 124.20, 118.21, 116.76, 115.47, 114.65, 112.08, 57.21, 55.28, 49.51, 39.12, 36.84, 36.81, 33.81, 31.63, 29.67, 29.46, 28.96, 26.91, 26.73, 24.53, 22.87, 22.56; HRMS $[M+H]^+$: 637.2903 (calculated for: $[C_{38}H_{42}ClN_4O_3]^+$ 637.2901

5.1.1.21. *N*-{8-[(6-chloro-1,2,3,4-tetrahydroacridin-9-yl)amino]octyl}-1-[(4-methoxyphenyl)methyl]-4-oxo-1,4-dihydroquinoline-3-carboxamide (**5u**)

Intermediate **4u** and BQCA reacted according to the general procedure to give the desired product as yellow solid (40 % yield): m.p. 54.6-56.7 °C; ^{1}H NMR (500 MHz, Chloroform-*d*) δ 10.05 (t, *J* = 5.7 Hz, 1H), 8.91 (s, 1H), 8.50 (dd, *J* = 8.1, 1.6 Hz, 1H), 7.90 (d, *J* = 9.1 Hz, 1H), 7.88 (d, *J* = 2.2 Hz, 1H), 7.64 – 7.58 (m, 1H), 7.43 (ddd, *J* = 8.1, 7.2, 6.1 Hz, 2H), 7.25 (dd, *J* = 9.1, 2.2 Hz, 1H), 7.12 – 7.07 (m, 2H), 6.88 – 6.82 (m, 2H), 5.38 (s, 2H), 3.77 (s, 3H), 3.51 – 3.44 (m, 4H), 3.05 – 2.99 (m, 2H), 2.69 – 2.64 (m, 2H), 1.93 – 1.88 (m, 4H), 1.70 – 1.61 (m, 4H), 1.48 – 1.30 (m, 8H); ^{13}C NMR (126 MHz, Chloroform-*d*) δ 176.84, 164.88, 159.72, 159.36, 150.91, 148.19, 148.17, 139.27, 133.98, 132.75, 128.09, 127.67, 127.40, 127.21, 127.18, 125.98, 125.06, 124.66, 124.18, 118.32, 116.75, 114.66, 112.12, 57.22, 55.30, 49.62, 39.19, 36.85, 33.95, 31.72, 29.54, 29.15, 26.91, 24.54, 22.62; HRMS $[M+H]^+$: 651.3081 (calculated for: $[C_{39}H_{44}ClN_4O_3]^+$ 651.3057

5.2. Cholinesterase Inhibition

The human erythrocyte acetylcholinesterase (*h*AChE; EC 3.1.1.7) and human plasmatic butyrylcholinesterase (*h*BChE; EC 3.1.1.8) inhibitory activity of the tested drugs was determined using Ellman´s method and is expressed as IC_{50}, i.e. concentration that reduces the cholinesterase activity by 50% [68]. 5,5´-Dithiobis(2-nitrobenzoic acid) (Ellman´s reagent, DTNB), KH_2PO_4, K_2HPO_4,

acetylthiocholine (ATCh), and butyrylthiocholine (BTCh), were purchased from Sigma-Aldrich, Prague, Czech Republic. For measuring purposes – polystyrene Nunc 96-well microplates with flat bottom shape (ThermoFisher Scientific, USA) were utilized. All the assays were carried out in 0.1 M KH_2PO_4/K_2HPO_4 buffer, pH 7.4. Enzyme solutions were prepared at 2.0 units/ mL in 2 mL aliquots. The assay medium (100 μL) consisted of 40 μL of 0.1 M phosphate buffer (pH 7.4), 20 μL of 0.01 M DTNB, 10 μL of enzyme, and 20 μL of 0.01 M substrate (ATCh iodide solution). Assay solutions with inhibitor (10^{-3} – 10^{-9} M) were pre-incubated 5 min. The reaction was started by immediate addition of 20 μL of substrate. The activity was determined by measuring the increase in absorbance at 412 nm at 37 °C at 2 min intervals - using a Multi-mode microplate reader Synergy 2 (Vermont, USA). Each concentration was assayed in triplicate. In vitro *h*BChE assay was similar with the method described above using BTCh as substrate instead of ATCh. Software GraphPad Prism 5 (San Diego, USA) was used for the statistical data evaluation.

5.3. Kinetic analysis

The kinetic study of *h*AChE was performed by using above mentioned Ellman's method [69–71]. The concentrations of **5p** used for the measurements were as follows: 1.00, 1.78, 3.16 and 5.62 nM. The values of V_{max} and K_m of the Michaelis-Menten kinetics as well as the values of K_i and $K_{i'}$ were calculated by non-linear regression from the substrate velocity curves. Linear regression was used for calculation of Lineweaver-Burk plots. All calculations were performed using GraphPad Prism software version 5.02 for Windows (San Diego, CA, USA).

5.4. Calcium mobilization assay

5.4.1. Cell culturing

Chinese hamster ovary cells (CHO-M1WT2, CRL-1984) stably expressing human recombinant M_1 mAChR (70 fmol/mg) were obtained from ATCC (Virginia, USA). Cells were cultured in the Ham´s F-12 medium with fetal bovine serum (10%) and geneticin (50 ng/mL). Cells were maintained at 37°C in the atmosphere of 5 % CO_2.

5.4.2. Fluo-4 NW Assay

Cells were plated out at density of ≈ 70,000 cells per well in 100 μL of medium, in a black-walled, clear-bottomed 96-well plate (Biotech, Czech Republic) and were grown overnight at 37 °C in the atmosphere of 5 % CO_2. The next day, the medium was removed leaving the cells adhering to the bottom. 100 μL of Fluo-4NW solution was added. Fluo-4NW solution was prepared according to manufacturer protocol, i.e. 10 mL of Hank´s balanced salt solution (HBSS buffer) and 100 µL of

probenecid solution were added to the dye mixture. Cells were incubated with the dye for 30 min at 37 °C/ 5 % CO_2 in the dark and 30 min at the room temperature.

The tested compounds were dissolved in DMSO and diluted 150 times by distilled water on the day of experiment. Further dilutions were prepared in the HBSS buffer and injected to a well, after 5s measurement of the baseline, where achieved the final tested concentration. The increase in fluorescence caused by the activation of the receptor was monitored for another 30s. The final concentration of DMSO in the well did not exceed 0.3 % (v/v).

The effect of novel compounds was compared to BQCA, a positive allosteric modulator standard. Cells were pre-incubated with the tested compound (10 μL/well) for 10 min and then EC_{20} of Oxo-M (30 nmol/l) was applied. Since the compounds inhibited the EC_{20} Oxo-M response, their inhibitory potency was then measured at EC_{80} Oxo-M (1 μmol/L). Ca^{2+} influx was measured by Synergy HT (Biotek, USA) at excitation and emission wavelength 485/20 nm and 528/20 nm respectively. All measurements were made at the room temperature ≈ 21 °C.

Oxo-M - evoked responses were quantified as the maximum response and expressed as a percentage of the average baseline values and normalized to the control. The first and the last wells received Oxo-M control and the mean was considered as 100% response in order to minimize time-depended errors (fading of responses), which were observed in the long- lasting experiments. Data were fitted using a standard four-parameter equation GraphPad Prism 5.0 (San Diego, USA) to generate graphs, IC_{50} and SEM.

5.5. Evaluation of cytotoxicity (MTT assay)

A hepatotoxicity of tested compounds was evaluated using the HepG2 cell line originally from human liver hepatocellular carcinoma (ATCC, USA). These cells were plated at density 17 × 10^3 per well in 96-well plate in Dulbecco's Modified Eagle's Medium (DMEM) (Gibco, USA) with 10% FBS (Gibco, USA) and incubated overnight. The incubation was performed under condition 37°C, 5% CO_2 and 80 – 95% air humidity. Stock solutions of tested compounds were prepared in dimethyl sulfoxide (DMSO) (Sigma –Aldrich, USA) and then diluted in DMEM medium. The final concentration of DMSO was less than 0.25%.

The cell viability was detected using (3-(4,5-dimethylthiazol-2-yl)-2,5-diphenyltetrazolium bromide) (MTT) assay [72] after 24 h of incubation with compounds. Then, medium was aspirated and 100 μL of MTT solution (0.5 mg/ml) in serum free of DMEM was added to each well. The cells were then incubated for one hour. The medium was then aspirated again and purple crystals of MTT formazan were dissolved in 100 μl DMSO under shaking. The absorbance was measured with a microplate reader (BioTek Instruments, USA) at a wavelength of 570 nm.

The IC_{50} values were calculated using four parametric nonlinear regression with statistic software GraphPad Prism 5.0 (San Diego, USA). Data were obtained from three independent experiments performed in triplicates. The IC_{50} values were expressed as mean ± SEM.

5.6. PAMPA assay

Penetration across the BBB is an essential property for compounds targeting the CNS. In order to predict passive blood-brain penetration of selected novel compounds, modification of the parallel artificial membrane permeation assay (PAMPA) has been used based on reported protocol [58,73]. The filter membrane of the donor plate was coated with PBL (Polar Brain Lipid, Avanti, USA) (4 μL of 20 mg/mL PBL in dodecane) and the acceptor well was filled with 300 μL of PBS pH 7.4 buffer (V_D). Tested compounds were dissolved (see below) to reach the final concentration 100 μM in the donor well. Concentration of DMSO did not exceed 0.5% (V/V) in the donor solution. 300 μL of the donor solution was added to the donor wells (V_A) and the donor filter plate was carefully put on the acceptor plate so that coated membrane was "in touch" with both donor solution and acceptor buffer. Test compound diffused from the donor well through the lipid membrane (Area=0.28 cm^2) to the acceptor well. The concentration of the drug in both donor and the acceptor wells was assessed after 3, 4, 5 and 6 hours of incubation in quadruplicate using the UV plate reader Synergy HT (Biotek, USA) at the maximum absorption wavelength of each compound. Concentration of the compounds was calculated from the standard curve and expressed as the permeability (*P*e) according the equation (1)

$$\log P_e = \log\left\{C \times -ln\left(1 - \frac{n_{acceptor}}{n_{total}}\right)\right\} \; where \; C = \left(\frac{V_D \times V_A}{(V_D + V_A) \times Area \times time}\right) \quad (1)$$

(1)

Compounds were firstly dissolved in the DMSO to make a stock solution. However, due to a low solubility of the stock in the PBS buffer, 1% pluronic (F-127, Sigma Aldrich) in the PBS pH 7.4 has been used for a donor solution. All the standard compounds, which have been tested for a correlation, were dissolved in this solvent and also in PBS.

*P*e values obtained in both solvents for standard drugs were statistically correlated by 2-way ANOVA followed by Bonferroni posttest in GraphPad Prism 5 (GraphPad Software Inc.). $p < 0,05$ is regarded as statistically significant.

5.7. Molecular modeling studies

From the online PDB database (www.pdb.org) models of *h*AChE (PDB ID: 4EY7, resolution: 2.35 Å) and *h*BChE (PDB ID: 4BDS, resolution: 2.10 Å) were downloaded and prepared for flexible molecular docking by MGL Tools utilities [60,61]. The preparation of this receptor involved removal of the surplus copies of the enzyme chains, non-bonded inhibitors, addition of polar hydrogens and merging of non-polar ones. Default Gasteiger charges were assigned to all atoms. Flexible parts of the enzymes were determined by a spherical selection of residues (R = 11 Å) approximately around the center of the active site. In the same points the centers of the grid box of 33 × 33 × 33 Å were positioned. The rotatable bonds in the flexible residues were detected automatically by AutoDock Tools 1.5.4 program. Given the limitation of the program used for flexible molecular docking, water molecules had to be removed from the system. The flexible receptor parts contained 40 residues for *h*AChE and 39 residues for *h*BChE. Following xyz coordinates of the grid box centers were applied: *h*AChE (10.698, -58.115, -23.192); *h*BChE (140.117, 122.247, 38.986). The studied ligands were firstly drawn in HyperChem 8.0, then manually protonated as suggested by MarvinSketch 6.2.0. software (http://www.chemaxon.com), geometrically optimized by semi-empirical quantum-chemistry PM3 method and stored as pdb files. The structures of the ligands were processed for docking in a similar way as abovementioned flexible parts of the receptor by AutoDock Tools 1.5.4 program. Molecular docking was carried out in AutoDock Vina 1.1.2 program utilizing computer resources of the Czech National Grid Infrastructure MetaCentrum. The search algorithm of AutoDock Vina efficiently combines a Markov chain Monte Carlo like method for the global search and a Broyden-Fletcher-Goldfarb-Shano gradient approach for the local search [64]. It is a type of memetic algorithm based on interleaving stochastic and deterministic calculations [74]. Each docking task was repeated 30 times with the exhaustiveness parameter set to 16, employing 16 CPU in parallel multithreading. From the obtained results, the solutions reaching the minimum predicted Gibbs binding energy were taken as the top-scoring modes. The graphic representations of the docked poses were rendered in PyMOL 1.3 (The PyMOL Molecular Graphics System, Version 1.5.0.4 Schrödinger, LLC.). 2D diagrams were generated using Discovery Studio Visualizer v16.1.0.15350 (Dassault Systèmes Biovia Corp., 2016, San Diego, USA).

Acknowledgment

The work was supported by the grant No. 16-08554S of the Grant Agency of the Czech Republic, by the institutional support: No. LO1611 with a financial support from the MEYS under the NPU I program, MH CZ - DRO (University Hospital Hradec Kralove, No. 00179906), "Long Term Development Plan" of the Ministry of Defence and by LTDP UHK. Also by the Ministry of Education, Youth and Sports of the Czech Republic under the Projects CESNET (Project No. LM2015042) and CERIT-Scientific Cloud (Project No. LM2015085) provided within the program Projects of Large Research, Development and Innovations Infrastructures.

Appendix A. Supplementary data

Supplementary data related to this article can be found at…

References

[1] J. Davis, R. Couch, Strategizing the Development of Alzheimer's Therapeutics, Adv. Alzheimers Dis. 03 (2014) 107. doi:10.4236/aad.2014.33011.

[2] W.J. Geldenhuys, M.B.H. Youdim, R.T. Carroll, C.J. Van der Schyf, The emergence of designed multiple ligands for neurodegenerative disorders, Prog. Neurobiol. 94 (2011) 347–359. doi:10.1016/j.pneurobio.2011.04.010.

[3] M. Valko, H. Morris, M.T.D. Cronin, Metals, toxicity and oxidative stress, Curr. Med. Chem. 12 (2005) 1161–1208.

[4] M. Horak, K. Holubova, E. Nepovimova, J. Krusek, M. Kaniakova, J. Korabecny, L. Vyklicky, K. Kuca, A. Stuchlik, J. Ricny, K. Vales, O. Soukup, The pharmacology of tacrine at N-methyl-d-aspartate receptors, Prog. Neuropsychopharmacol. Biol. Psychiatry. 75 (2017) 54–62. doi:10.1016/j.pnpbp.2017.01.003.

[5] R. Leurs, R.A. Bakker, H. Timmerman, I.J.P. de Esch, The histamine H3 receptor: from gene cloning to H3 receptor drugs, Nat. Rev. Drug Discov. 4 (2005) 107–120. doi:10.1038/nrd1631.

[6] R.T. Bartus, R.L. Dean, B. Beer, A.S. Lippa, The cholinergic hypothesis of geriatric memory dysfunction, Science. 217 (1982) 408–414.

[7] R. Briggs, S.P. Kennelly, D. O'Neill, Drug treatments in Alzheimer's disease, Clin. Med. Lond. Engl. 16 (2016) 247–253. doi:10.7861/clinmedicine.16-3-247.

[8] A.C. Foster, R. Gill, L.L. Iversen, J.A. Kemp, E.H. Wong, G.N. Woodruff, Therapeutic potential of NMDA receptor antagonists as neuroprotective agents, Prog. Clin. Biol. Res. 361 (1990) 301–329.

[9] E. Giacobini, Invited Review Cholinesterase inhibitors for Alzheimer's disease therapy: from tacrine to future applications, Neurochem. Int. 32 (1998) 413–419. doi:10.1016/S0197-0186(97)00124-1.

[10] K. Spilovska, J. Korabecny, E. Nepovimova, R. Dolezal, E. Mezeiova, O. Soukup, K. Kuca, Multitarget Tacrine Hybrids with Neuroprotective Properties to Confront Alzheimer's Disease, Curr. Top. Med. Chem. 17 (2017) 1006–1026. doi:10.2174/1568026605666160927152728.

[11] J. Korabecny, R. Dolezal, P. Cabelova, A. Horova, E. Hruba, J. Ricny, L. Sedlacek, E. Nepovimova, K. Spilovska, M. Andrs, K. Musilek, V. Opletalova, V. Sepsova, D. Ripova, K. Kuca, 7-MEOTA-donepezil like compounds as cholinesterase inhibitors: Synthesis, pharmacological evaluation, molecular modeling and QSAR studies, Eur. J. Med. Chem. 82 (2014) 426–438. doi:10.1016/j.ejmech.2014.05.066.

[12] J. Jeřábek, E. Uliassi, L. Guidotti, J. Korábečný, O. Soukup, V. Sepsova, M. Hrabinova, K. Kuča, M. Bartolini, L.E. Peña-Altamira, S. Petralla, B. Monti, M. Roberti, M.L. Bolognesi, Tacrine-

resveratrol fused hybrids as multi-target-directed ligands against Alzheimer's disease, Eur. J. Med. Chem. 127 (2017) 250–262. doi:10.1016/j.ejmech.2016.12.048.

[13] A.I. Levey, C.A. Kitt, W.F. Simonds, D.L. Price, M.R. Brann, Identification and localization of muscarinic acetylcholine receptor proteins in brain with subtype-specific antibodies, J. Neurosci. Off. J. Soc. Neurosci. 11 (1991) 3218–3226.

[14] A. Fisher, D.M. Michaelson, R. Brandeis, R. Haring, S. Chapman, Z. Pittel, M1 muscarinic agonists as potential disease-modifying agents in Alzheimer's disease. Rationale and perspectives, Ann. N. Y. Acad. Sci. 920 (2000) 315–320.

[15] M. Decker, U. Holzgrabe, M1 muscarinic cetylcholine receptor allosteric modulators as potential therapeutic opportunities for treating Alzheimer's disease, Med. Chem. Commun. 3 (2012) 752–762. doi:10.1039/C2MD20025B.

[16] A. Fisher, M1 muscarinic agonists target major hallmarks of Alzheimer's disease--the pivotal role of brain M1 receptors, Neurodegener. Dis. 5 (2008) 237–240. doi:10.1159/000113712.

[17] A.A. Davis, J.J. Fritz, J. Wess, J.J. Lah, A.I. Levey, Deletion of M1 muscarinic acetylcholine receptors increases amyloid pathology in vitro and in vivo, J. Neurosci. Off. J. Soc. Neurosci. 30 (2010) 4190–4196. doi:10.1523/JNEUROSCI.6393-09.2010.

[18] S. Jiang, Y. Wang, Q. Ma, A. Zhou, X. Zhang, Y. Zhang, M1 muscarinic acetylcholine receptor interacts with BACE1 and regulates its proteosomal degradation, Neurosci. Lett. 515 (2012) 125–130. doi:10.1016/j.neulet.2012.03.026.

[19] J.C. Tarr, M.L. Turlington, P.R. Reid, T.J. Utley, D.J. Sheffler, H.P. Cho, R. Klar, T. Pancani, M.T. Klein, T.M. Bridges, R.D. Morrison, A.L. Blobaum, Z. Xiang, J.S. Daniels, C.M. Niswender, P.J. Conn, M.R. Wood, C.W. Lindsley, Targeting selective activation of M(1) for the treatment of Alzheimer's disease: further chemical optimization and pharmacological characterization of the M(1) positive allosteric modulator ML169, ACS Chem. Neurosci. 3 (2012) 884–895. doi:10.1021/cn300068s.

[20] J. Nunan, D.H. Small, Regulation of APP cleavage by alpha-, beta- and gamma-secretases, FEBS Lett. 483 (2000) 6–10.

[21] J.K. Shirey, A.E. Brady, P.J. Jones, A.A. Davis, T.M. Bridges, J.P. Kennedy, S.B. Jadhav, U.N. Menon, Z. Xiang, M.L. Watson, E.P. Christian, J.J. Doherty, M.C. Quirk, D.H. Snyder, J.J. Lah, A.I. Levey, M.M. Nicolle, C.W. Lindsley, P.J. Conn, A selective allosteric potentiator of the M1 muscarinic acetylcholine receptor increases activity of medial prefrontal cortical neurons and restores impairments in reversal learning, J. Neurosci. Off. J. Soc. Neurosci. 29 (2009) 14271–14286. doi:10.1523/JNEUROSCI.3930-09.2009.

[22] L. Ma, M.A. Seager, M. Seager, M. Wittmann, M. Jacobson, D. Bickel, M. Burno, K. Jones, V.K. Graufelds, G. Xu, M. Pearson, A. McCampbell, R. Gaspar, P. Shughrue, A. Danziger, C. Regan, R. Flick, D. Pascarella, S. Garson, S. Doran, C. Kreatsoulas, L. Veng, C.W. Lindsley, W. Shipe, S. Kuduk, C. Sur, G. Kinney, G.R. Seabrook, W.J. Ray, Selective activation of the M1 muscarinic acetylcholine receptor achieved by allosteric potentiation, Proc. Natl. Acad. Sci. U. S. A. 106 (2009) 15950–15955. doi:10.1073/pnas.0900903106.

[23] E. Nepovimova, J. Korabecny, R. Dolezal, K. Babkova, A. Ondrejicek, D. Jun, V. Sepsova, A. Horova, M. Hrabinova, O. Soukup, N. Bukum, P. Jost, L. Muckova, J. Kassa, D. Malinak, M. Andrs, K. Kuca, Tacrine-Trolox Hybrids: A Novel Class of Centrally Active, Nonhepatotoxic Multi-Target-Directed Ligands Exerting Anticholinesterase and Antioxidant Activities with Low In Vivo Toxicity, J. Med. Chem. 58 (2015) 8985–9003. doi:10.1021/acs.jmedchem.5b01325.

[24] Z. Gazova, O. Soukup, V. Sepsova, K. Siposova, L. Drtinova, P. Jost, K. Spilovska, J. Korabecny, E. Nepovimova, D. Fedunova, M. Horak, M. Kaniakova, Z.-J. Wang, A.K. Hamouda, K. Kuca, Multi-target-directed therapeutic potential of 7-methoxytacrine-adamantylamine heterodimers in the Alzheimer's disease treatment, Biochim. Biophys. Acta. 1863 (2017) 607–619. doi:10.1016/j.bbadis.2016.11.020.

[25] M. Recanatini, A. Cavalli, F. Belluti, L. Piazzi, A. Rampa, A. Bisi, S. Gobbi, P. Valenti, V. Andrisano, M. Bartolini, V. Cavrini, SAR of 9-amino-1,2,3,4-tetrahydroacridine-based acetylcholinesterase

inhibitors: synthesis, enzyme inhibitory activity, QSAR, and structure-based CoMFA of tacrine analogues, J. Med. Chem. 43 (2000) 2007–2018.

[26] O. Soukup, D. Jun, J. Zdarova-Karasova, J. Patocka, K. Musilek, J. Korabecny, J. Krusek, M. Kaniakova, V. Sepsova, J. Mandikova, F. Trejtnar, M. Pohanka, L. Drtinova, M. Pavlik, G. Tobin, K. Kuca, A resurrection of 7-MEOTA: a comparison with tacrine, Curr. Alzheimer Res. 10 (2013) 893–906.

[27] J. Patocka, D. Jun, K. Kuca, Possible role of hydroxylated metabolites of tacrine in drug toxicity and therapy of Alzheimer's disease, Curr. Drug Metab. 9 (2008) 332–335.

[28] A. Adem, Putative mechanisms of action of tacrine in Alzheimer's disease, Acta Neurol. Scand. Suppl. 139 (1992) 69–74.

[29] W.K. Summers, K.R. Kaufman, F. Altman, J.M. Fischer, THA--a review of the literature and its use in treatment of five overdose patients, Clin. Toxicol. 16 (1980) 269–281. doi:10.3109/15563658008989949.

[30] A.J. Wagstaff, D. McTavish, Tacrine. A review of its pharmacodynamic and pharmacokinetic properties, and therapeutic efficacy in Alzheimer's disease, Drugs Aging. 4 (1994) 510–540.

[31] L. Fang, S. Jumpertz, Y. Zhang, D. Appenroth, C. Fleck, K. Mohr, C. Tränkle, M. Decker, Hybrid molecules from xanomeline and tacrine: enhanced tacrine actions on cholinesterases and muscarinic M1 receptors, J. Med. Chem. 53 (2010) 2094–2103. doi:10.1021/jm901616h.

[32] G.W. Amarante, M. Benassi, R.N. Pascoal, M.N. Eberlin, F. Coelho, Mechanism and synthesis of pharmacologically active quinolones from Morita–Baylis–Hillman adducts, Tetrahedron. 66 (2010) 4370–4376. doi:10.1016/j.tet.2010.04.018.

[33] R.G. Gould, W.A. Jacobs, The Synthesis of Certain Substituted Quinolines and 5,6-Benzoquinolines, J. Am. Chem. Soc. 61 (1939) 2890–2895. doi:10.1021/ja01265a088.

[34] E. Nepovimova, E. Uliassi, J. Korabecny, L.E. Peña-Altamira, S. Samez, A. Pesaresi, G.E. Garcia, M. Bartolini, V. Andrisano, C. Bergamini, R. Fato, D. Lamba, M. Roberti, K. Kuca, B. Monti, M.L. Bolognesi, Multitarget Drug Design Strategy: Quinone–Tacrine Hybrids Designed To Block Amyloid-β Aggregation and To Exert Anticholinesterase and Antioxidant Effects, J. Med. Chem. 57 (2014) 8576–8589. doi:10.1021/jm5010804.

[35] B. Drukarch, K.S. Kits, E.G. Van der Meer, J.C. Lodder, J.C. Stoof, 9-Amino-1,2,3,4-tetrahydroacridine (THA), an alleged drug for the treatment of Alzheimer's disease, inhibits acetylcholinesterase activity and slow outward K+ current, Eur. J. Pharmacol. 141 (1987) 153–157.

[36] K. Spilovska, J. Korabecny, V. Sepsova, D. Jun, M. Hrabinova, P. Jost, L. Muckova, O. Soukup, J. Janockova, T. Kucera, R. Dolezal, E. Mezeiova, D. Kaping, K. Kuca, Novel Tacrine-Scutellarin Hybrids as Multipotent Anti-Alzheimer's Agents: Design, Synthesis and Biological Evaluation, Mol. Basel Switz. 22 (2017). doi:10.3390/molecules22061006.

[37] H. Dvir, I. Silman, M. Harel, T.L. Rosenberry, J.L. Sussman, Acetylcholinesterase: From 3D Structure to Function, Chem. Biol. Interact. 187 (2010) 10–22. doi:10.1016/j.cbi.2010.01.042.

[38] Y.P. Pang, P. Quiram, T. Jelacic, F. Hong, S. Brimijoin, Highly potent, selective, and low cost bis-tetrahydroaminacrine inhibitors of acetylcholinesterase. Steps toward novel drugs for treating Alzheimer's disease, J. Biol. Chem. 271 (1996) 23646–23649.

[39] M.A. Ceschi, J.S. da Costa, J.P.B. Lopes, V.S. Câmara, L.F. Campo, A.C. de A. Borges, C.A.S. Gonçalves, D.F. de Souza, E.L. Konrath, A.L.M. Karl, I.A. Guedes, L.E. Dardenne, Novel series of tacrine-tianeptine hybrids: Synthesis, cholinesterase inhibitory activity, S100B secretion and a molecular modeling approach, Eur. J. Med. Chem. 121 (2016) 758–772. doi:10.1016/j.ejmech.2016.06.025.

[40] J. Korabecny, M. Andrs, E. Nepovimova, R. Dolezal, K. Babkova, A. Horova, D. Malinak, E. Mezeiova, L. Gorecki, V. Sepsova, M. Hrabinova, O. Soukup, D. Jun, K. Kuca, 7-Methoxytacrine-p-Anisidine Hybrids as Novel Dual Binding Site Acetylcholinesterase Inhibitors for Alzheimer's Disease Treatment, Mol. Basel Switz. 20 (2015) 22084–22101. doi:10.3390/molecules201219836.

[41] Y. Wang, H. Wang, H. Chen, AChE Inhibition-based Multi-target-directed Ligands, a Novel Pharmacological Approach for the Symptomatic and Disease-modifying Therapy of Alzheimer's Disease, Curr. Neuropharmacol. 14 (2016) 364–375.

[42] M.-M. Mesulam, A. Guillozet, P. Shaw, A. Levey, E.G. Duysen, O. Lockridge, Acetylcholinesterase knockouts establish central cholinergic pathways and can use butyrylcholinesterase to hydrolyze acetylcholine, Neuroscience. 110 (2002) 627–639.

[43] J. Hartmann, C. Kiewert, E.G. Duysen, O. Lockridge, N.H. Greig, J. Klein, Excessive hippocampal acetylcholine levels in acetylcholinesterase-deficient mice are moderated by butyrylcholinesterase activity, J. Neurochem. 100 (2007) 1421–1429. doi:10.1111/j.1471-4159.2006.04347.x.

[44] S. Darvesh, D.A. Hopkins, Differential distribution of butyrylcholinesterase and acetylcholinesterase in the human thalamus, J. Comp. Neurol. 463 (2003) 25–43. doi:10.1002/cne.10751.

[45] P. Muñoz-Ruiz, L. Rubio, E. García-Palomero, I. Dorronsoro, M. del Monte-Millán, R. Valenzuela, P. Usán, C. de Austria, M. Bartolini, V. Andrisano, A. Bidon-Chanal, M. Orozco, F.J. Luque, M. Medina, A. Martínez, Design, Synthesis, and Biological Evaluation of Dual Binding Site Acetylcholinesterase Inhibitors: New Disease-Modifying Agents for Alzheimer's Disease, J. Med. Chem. 48 (2005) 7223–7233. doi:10.1021/jm0503289.

[46] M. Recanatini, A. Cavalli, Acetylcholinesterase inhibitors in the context of therapeutic strategies to combat Alzheimer's disease, Expert Opin. Ther. Pat. 12 (2002) 1853–1865. doi:10.1517/13543776.12.12.1853.

[47] M. Recanatini, A. Cavalli, F. Belluti, L. Piazzi, A. Rampa, A. Bisi, S. Gobbi, P. Valenti, V. Andrisano, M. Bartolini, V. Cavrini, SAR of 9-Amino-1,2,3,4-tetrahydroacridine-Based Acetylcholinesterase Inhibitors: Synthesis, Enzyme Inhibitory Activity, QSAR, and Structure-Based CoMFA of Tacrine Analogues, J. Med. Chem. 43 (2000) 2007–2018. doi:10.1021/jm990971t.

[48] N.C. Inestrosa, J.P. Sagal, M. Colombres, Acetylcholinesterase interaction with Alzheimer amyloid beta, Subcell. Biochem. 38 (2005) 299–317.

[49] N.C. Inestrosa, A. Alvarez, C.A. Pérez, R.D. Moreno, M. Vicente, C. Linker, O.I. Casanueva, C. Soto, J. Garrido, Acetylcholinesterase accelerates assembly of amyloid-beta-peptides into Alzheimer's fibrils: possible role of the peripheral site of the enzyme, Neuron. 16 (1996) 881–891.

[50] S. Nochi, N. Asakawa, T. Sato, Kinetic study on the inhibition of acetylcholinesterase by 1-benzyl-4-[(5,6-dimethoxy-1-indanon)-2-yl]methylpiperidine hydrochloride (E2020), Biol. Pharm. Bull. 18 (1995) 1145–1147.

[51] M. Bartolini, C. Bertucci, V. Cavrini, V. Andrisano, beta-Amyloid aggregation induced by human acetylcholinesterase: inhibition studies, Biochem. Pharmacol. 65 (2003) 407–416.

[52] E.K. Perry, C.J. Smith, J.A. Court, J.R. Bonham, M. Rodway, J.R. Atack, Interaction of 9-amino-1,2,3,4-tetrahydroaminoacridine (THA) with human cortical nicotinic and muscarinic receptor binding in vitro, Neurosci. Lett. 91 (1988) 211–216.

[53] J. Wess, Allosteric binding sites on muscarinic acetylcholine receptors, Mol. Pharmacol. 68 (2005) 1506–1509. doi:10.1124/mol.105.019141.

[54] R. Messerer, C. Dallanoce, C. Matera, S. Wehle, L. Flammini, B. Chirinda, A. Bock, M. Irmen, C. Tränkle, E. Barocelli, M. Decker, C. Sotriffer, M.D. Amici, U. Holzgrabe, Novel bipharmacophoric inhibitors of the cholinesterases with affinity to the muscarinic receptors M1 and M2, MedChemComm. 8 (2017) 1346–1359. doi:10.1039/C7MD00149E.

[55] D.J. Ames, P.S. Bhathal, B.M. Davies, J.R. Fraser, Hepatotoxicity of tetrahydroaminoacridine, Lancet Lond. Engl. 1 (1988) 887.

[56] W.K. Summers, A.L. Koehler, G.M. Marsh, K. Tachiki, A. Kling, Long-term hepatotoxicity of tacrine, Lancet Lond. Engl. 1 (1989) 729.

[57] Y. Dgachi, H. Martin, A. Bonet, M. Chioua, I. Iriepa, I. Moraleda, F. Chabchoub, J. Marco-Contelles, L. Ismaili, Synthesis and biological assessment of racemic

benzochromenopyrimidinetriones as promising agents for Alzheimer's disease therapy, Future Med. Chem. (2017). doi:10.4155/fmc-2017-0004.

[58] L. Di, E.H. Kerns, K. Fan, O.J. McConnell, G.T. Carter, High throughput artificial membrane permeability assay for blood-brain barrier, Eur. J. Med. Chem. 38 (2003) 223–232.

[59] W.M. Pardridge, Drug transport across the blood–brain barrier, J. Cereb. Blood Flow Metab. 32 (2012) 1959–1972. doi:10.1038/jcbfm.2012.126.

[60] J. Cheung, M.J. Rudolph, F. Burshteyn, M.S. Cassidy, E.N. Gary, J. Love, M.C. Franklin, J.J. Height, Structures of human acetylcholinesterase in complex with pharmacologically important ligands, J. Med. Chem. 55 (2012) 10282–10286. doi:10.1021/jm300871x.

[61] F. Nachon, E. Carletti, C. Ronco, M. Trovaslet, Y. Nicolet, L. Jean, P.-Y. Renard, Crystal structures of human cholinesterases in complex with huprine W and tacrine: elements of specificity for anti-Alzheimer's drugs targeting acetyl- and butyryl-cholinesterase, Biochem. J. 453 (2013) 393–399. doi:10.1042/BJ20130013.

[62] A. Nordberg, C. Ballard, R. Bullock, T. Darreh-Shori, M. Somogyi, A review of butyrylcholinesterase as a therapeutic target in the treatment of Alzheimer's disease, Prim. Care Companion CNS Disord. 15 (2013). doi:10.4088/PCC.12r01412.

[63] M. Bajda, A. Więckowska, M. Hebda, N. Guzior, C.A. Sotriffer, B. Malawska, Structure-based search for new inhibitors of cholinesterases, Int. J. Mol. Sci. 14 (2013) 5608–5632. doi:10.3390/ijms14035608.

[64] O. Trott, A.J. Olson, AutoDock Vina: improving the speed and accuracy of docking with a new scoring function, efficient optimization, and multithreading, J. Comput. Chem. 31 (2010) 455–461. doi:10.1002/jcc.21334.

[65] R. Dolezal, J. Korabecny, D. Malinak, J. Honegr, K. Musilek, K. Kuca, Ligand-based 3D QSAR analysis of reactivation potency of mono- and bis-pyridinium aldoximes toward VX-inhibited rat acetylcholinesterase, J. Mol. Graph. Model. 56 (2015) 113–129. doi:10.1016/j.jmgm.2014.11.010.

[66] K. Spilovska, J. Korabecny, A. Horova, K. Musilek, E. Nepovimova, L. Drtinova, Z. Gazova, K. Siposova, R. Dolezal, D. Jun, K. Kuca, Design, synthesis and in vitro testing of 7-methoxytacrine-amantadine analogues: a novel cholinesterase inhibitors for the treatment of Alzheimer's disease, Med. Chem. Res. (2015) 1–11. doi:10.1007/s00044-015-1316-x.

[67] S. Hamulakova, L. Janovec, M. Hrabinova, K. Spilovska, J. Korabecny, P. Kristian, K. Kuca, J. Imrich, Synthesis and biological evaluation of novel tacrine derivatives and tacrine-coumarin hybrids as cholinesterase inhibitors, J. Med. Chem. 57 (2014) 7073–7084. doi:10.1021/jm5008648.

[68] G.L. Ellman, K.D. Courtney, V. Andres, R.M. Feather-Stone, A new and rapid colorimetric determination of acetylcholinesterase activity, Biochem. Pharmacol. 7 (1961) 88–95.

[69] G.L. Ellman, K.D. Courtney, V. Andres, R.M. Feather-Stone, A new and rapid colorimetric determination of acetylcholinesterase activity, Biochem. Pharmacol. 7 (1961) 88–95.

[70] M. Pohanka, J.Z. Karasova, K. Kuca, J. Pikula, O. Holas, J. Korabecny, J. Cabal, Colorimetric dipstick for assay of organophosphate pesticides and nerve agents represented by paraoxon, sarin and VX, Talanta. 81 (2010) 621–624. doi:10.1016/j.talanta.2009.12.052.

[71] V. Sepsova, J.Z. Karasova, J. Korabecny, R. Dolezal, F. Zemek, B.J. Bennion, K. Kuca, Oximes: inhibitors of human recombinant acetylcholinesterase. A structure-activity relationship (SAR) study, Int. J. Mol. Sci. 14 (2013) 16882–16900. doi:10.3390/ijms140816882.

[72] T. Mosmann, Rapid colorimetric assay for cellular growth and survival: Application to proliferation and cytotoxicity assays, J. Immunol. Methods. 65 (1983) 55–63. doi:10.1016/0022-1759(83)90303-4.

[73] L.F.N. Lemes, G. de Andrade Ramos, A.S. de Oliveira, F.M.R. da Silva, G. de Castro Couto, M. da Silva Boni, M.J.R. Guimarães, I.N.O. Souza, M. Bartolini, V. Andrisano, P.C. do Nascimento Nogueira, E.R. Silveira, G.D. Brand, O. Soukup, J. Korábečný, N.C. Romeiro, N.G. Castro, M.L. Bolognesi, L.A.S. Romeiro, Cardanol-derived AChE inhibitors: Towards the development of dual

binding derivatives for Alzheimer's disease, Eur. J. Med. Chem. 108 (2016) 687–700. doi:10.1016/j.ejmech.2015.12.024.

[74] B. Liu, L. Wang, Y.-H. Jin, An effective PSO-based memetic algorithm for flow shop scheduling, IEEE Trans. Syst. Man Cybern. Part B Cybern. Publ. IEEE Syst. Man Cybern. Soc. 37 (2007) 18–27.

Highlights:

- Tacrine-BQCA hybrids inhibit both cholinesterases in nanomolar concentrations
- Tacrine moiety ensures interaction with cholinesterases
- Tacrine-BQCA hybrids effectively inhibit muscarinic M1 receptor
- Some tacrine-BQCA derivatives are predicted to cross blood-brain barrier